Double Emulsion Mucoadhesive Nanoparticles for Hydrophilic Ocular Drug Delivery

by

Noor El-Huda Bahsoun

A thesis

presented to the University of Waterloo

in fulfillment of the

thesis requirement for the degree of

Masters of Applied Science

in

Chemical Engineering (Nanotechnology)

Waterloo, Ontario, Canada, 2018

Authors Declaration

I hereby declare that I am the sole author of this thesis. This is a true copy of the thesis, including any required final revisions, as accepted by my examiners. I understand that my thesis may be made electronically available to the public.

Abstract

Common eye diseases such as conjunctivitis affect around 6 million people annually. Although eye drops are the most common treatment for these diseases, topical administration is limited by low ocular bioavailability due to lachrymal drainage, low drug permeability across the corneal epithelium, and low drug stability as a result of tear dilution and turnover. This results in over 95% of the drugs applied through eye drops to be quickly cleared away. Consequently, patients struggle with the multiple daily applications required and the resulting side effects.

In order to overcome these barriers and to increase contact time of drugs on the surface of the eye, several nanoparticle (NP) technologies have been developed for the delivery of drugs to our systems like liposomes, hydrogels, microparticles, micelles, implants...etc. NP surfaces can be tuned to achieve specific properties such as binding affinity towards the ocular surface. NPs can also carry a large amount of drugs and release them in a sustained manner over a long period. Due to their small size, NPs do not cause abrasive sensations on the eye upon patient application. There is no one technology that is suitable for any drug to any site, however biodegradable colloidal systems appear to be the most advantageous. Their popularity stems from their biocompatibility with ocular tissues, high encapsulation efficiency, sustained release, and ability to degrade into non-toxic by-products that are safely cleared from ocular tissues. With these unique advantages, NP drug carriers may drastically improve patient compliance while reducing side effects.

Research conducted in the Frank Gu Research Group suggests that NP drug carriers are capable of circumventing corneal clearance mechanisms by manipulating the surface functionalization of polymeric nanoparticles (NPs) such that they can interact with the ocular mucosa. In view of this background, this thesis was aimed at exploring the potential of mucoadhesive NPs (MNPs) to encapsulate hydrophilic drugs in the core of the NP, while maintaining mucoadhesive functionality in the shell of the NP. We developed a novel approach to formulate a double emulsion mucoadhesive nanoparticle (DE MNP) system to deliver hydrophilic molecules.

Double emulsions allow us to generate a vesicle-like structure of hydrophilic interior and hydrophilic exterior and have been successful as nanoparticle drug carriers in the past. Most double emulsions utilize PLGA to make up the primary emulsion because it is a biodegradable and biocompatible polymer that has the ability to degrade into non-toxic by-products (lactic acid and glycolic acid) that are metabolized by the human body. The novelty in the DE MNP method involves using PLA-Dex-PBA in the outer emulsion, rather than common stabilizers such as PVA and Tween. The amphiphilic characteristics of PLA-Dex-PBA will arrange on the surface of PLGA emulsions with PLA facing the oil phase and Dex-PBA facing the exterior of the particle, making up the surface of DE MNPs. The PBA

moieties on the surface of DE MNPs can covalently target the sialic acid moieties that are abundant on the ocular mucous membrane and avoid rapid clearance. DE MNPs form the foundation of the ocular drug delivery platform developed in this thesis, using fluorescein isothiocyanate dextran (FITC-Dex), a commercially used fluorescent dye, as the model drug to determine the capability of DE MNPs to encapsulate and release hydrophilic molecules. DE MNPs were first evaluated for size and morphology. They demonstrated sizes in the sub-200 nm range, nearly double the size of PLA-Dex-PBA MNP micelles. Their spherical shell/vesicle conformation was confirmed by static light scattering and TEM, and remained stable and unchanged with the addition of model FITC-Dex. DE MNPs demonstrated encapsulation of FITC-Dex up to 87 wt%, and sustained release for up to 7 days *in vitro*, showing their potential as a long-term eye drop delivery platform.

In vitro mucoadhesion study as a proof of concept demonstration of PBA on DE MNPs' surfaces was demonstrated by studying the binding kinetics of PBA to sialic acid through the Stern-Volmer equation. The K_A value for DE MNPs with sialic acid was determined to be 107.83 M-1, which is far higher than the literature values for PBA-SA. This gave confidence to the presence of PBA on the surface of DE MNPs. Next, we proceeded to attempt to demonstrate this mucoadhesion using *in vivo* models. FITC-Dex was encapsulated in the NPs and administered to rabbit eyes to track its ocular retention. FITC-Dex delivered DE MNPs showed ocular retention for no longer than 3 hours on rabbit eyes; this trend was also seen for free FITC-Dex.

Povidone-Iodine (PVP-I), an inexpensive and commercially available drug commonly used to treat ocular bacterial infections, was encapsulated and evaluated for bactericidal activity upon release from DE MNPs. DE MNPs revealed that that encapsulation of the drug did not change the properties of the drug, and also confirmed that the amount of drug being encapsulated (1% w/v) in DE MNPs, is a sufficient concentration to elicit antimicrobial activity, and better than current formulations such as Betadine® which uses 5%w/v PVP-I for treatment of ocular infection.

This thesis demonstrates the development process of DE MNPs as topical ocular drug delivery systems for hydrophilic drugs. DE MNPs demonstrated delivery of a clinically relevant dosage of PVP-I, controlled release of therapeutics over prolonged period of time, and mucoadhesive properties *in vitro*. These DE mucoadhesive NPs show significant promise as a long-term topical ocular hydrophilic drug delivery system that significantly reduces the dose and the administration frequency of the eye drops while minimizing side effects.

Acknowledgements

First and foremost, I'd like to extend my sincerest thanks to my supervisor Dr. Frank Gu for allowing this biologist the opportunity to exercise the engineer inside, and for being an incredible mentor. Your guidance and encouragement these past two years has kept me sane and helped make my overwhelming tasks seem less so.

I would also like to thank my colleague and friend Dr. Shengyan Liu. You taught me to be an independent researcher, to be confident in my abilities as a lab researcher and most importantly to think outside the box. Thank you for your help and support through my syntheses that took months to work and for guiding me through both my failures and my successes.

Next, I would like to thank my coop students Sabrina Zuccaro, Soung-jae Bong, and Katie Kobernyk for their hard work and contributions to this project. Your presence in the lab made it a pleasure to come in everyday to bounce ideas off of each other and work together. I am especially grateful for the funding and support received from the University of Waterloo, and the National Sciences and Engineering Research Council of Canada.

Last but not least, I would like to thank my family and friends, for their patience, support, and pride throughout my graduate degree. Every time I started thinking I wasn't cut out for engineering, you helped me see otherwise. I know you don't understand the scientific jargon, but thank you for listening to my excitement and complaints anyways!

Dedication

To my brother, Mohamad-Ali Bahsoun.

I wouldn't be an engineer today without you.

Table of Contents

List of Figures

List of Tables

List of Equations

List of Abbreviations

DE: Double Emulsion

MNP: Mucoadhesive Nanoparticle

NP: Nanoparticle

PLA: Poly(lactic acid)

PLGA: Poly(lactic-co-glycolic acid)

aPBA: 3-aminophenylboronic acid

SA: Sialic acid

FITC-Dex: Fluorescein isothiocyanate dextran

PVP-I: Polyvinylpyrrolidone-Iodine or Povidone-Iodine

DCM: Dichloromethane

DMSO: Dimethyl sulfoxide

SPAN80: Sorbitan monooleate

MilliQ: Millipore H_2O

STF: Simulated Tear Fluid

DLS: Dynamic Light Scattering

SLS: Static Light Scattering

TEM: Transmission electron microscopy

UV-Vis: Ultraviolet-visible spectroscopy

EE: Encapsulation efficiency

DL: Drug loading

w/v: Weight per volume

w/w: Weight per weight

PTA: Phosphotungstic acid

R_g: Radius of gyration

R_h: Hydrodynamic radius

PDI: Polydispersity Index

E coli: Escherichia coli

nm: Nanometer

mg: Milligram

μg: Microgram

mL: Milliliter

W/O/W: Water-in-oil-in-water

Chapter 1
Introduction

1.1 Overview

Ocular drug delivery remains among the most challenging approaches to administering therapeutic agents due to the complexity of the physiological environments surrounding the eye. The eye has many mechanisms in place to protect it from both its external and internal environments [6] and drug delivery to this sensitive and sophisticated organ can be challenging since the eye's protective barriers need to be circumvented if one is to establish therapeutically effective drug concentrations in the intraocular tissues [7]. These barriers come in the form of physiochemical limitations of the biopharmaceuticals themselves, the physiology and anatomy of the eye, and the formulation conditions of the carriers for these protein therapeutics.

Topical administration in the form of ophthalmic drops is the most popular and preferred route to treat anterior segment diseases due to its non- invasiveness and ease of application. However, the efficiency of topical drug administration is limited by low ocular bioavailability due to rapid drainage, low drug permeability across the corneal epithelium, and low drug stability as a result of tear dilution and turnover; as a result, approximately 95% of the administered drugs are cleared within ten minutes of administration [6]. Therefore, topical formulations typically require frequent administration, which increases the risk of side effects, and leads to lower patient compliance.

Nanocarrier-based ocular drug delivery systems appear to be the most promising tool for targeted drug delivery. The use of nanoparticles (NPs) as drug carriers represents a significant improvement over traditional oral and intravenous methods of administration. It protects drugs from degradation and reduces the dosage of the drug administered, thus improving drug efficacy and efficiency in addition to limiting unwanted side effects [7]. Furthermore, NP drug carriers have the potential to overcome challenges posed by current eye drop formulations. These carriers have high surface area-to-volume ratios due to their small size, which provide an optimal template for targeted drug delivery and improves patient comfort because it is non-abrasive on the surface of the eye. NP drug carriers have already demonstrated high diffusivity across membranes such as the corneal epithelium due to their small size [2], and they have been found to improve the stability of drugs through encapsulation [2] as well as release of the encapsulated therapeutics in a controlled and sustained manner.

Currently, a variety of NP drug delivery platforms have been investigated including, but not limited to, liposomes, micelles, nanospheres, nanocapsules, polymerosomes, and carbon nanotubes.

Research conducted in the Frank Gu Research Group suggests that NP drug carriers are capable of circumventing corneal clearance mechanisms by manipulating the surface functionalization of polymeric NPs such that they can interact with the ocular mucosa [2].

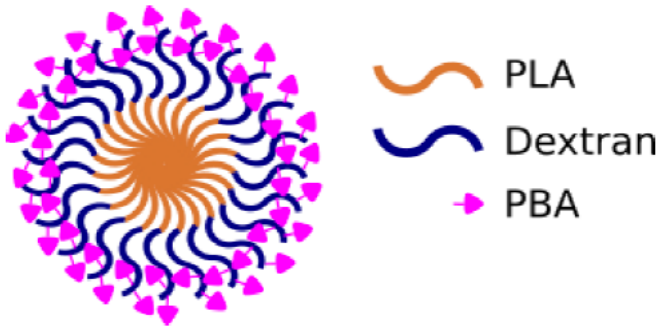

Figure 1.1 Schematic of MNPs with hydrophobic PLA, hydrophilic dextran, and surface-functionalized PBA grafts.

The Frank Gu Research Group has developed mucoadhesive nanoparticles (MNPs) for targeted drug delivery to the ocular surface. The presence of a mucus layer in the anterior segment of the eye allows MNPs to prolong the retention of the topically administered drug formulations by binding to sialic acid - an abundant terminal sugar on the mucus membrane of the eye. These MNPs are polymeric self-assembled micelles that contain a hydrophobic core of poly(lactic acid) (PLA), a hydrophilic shell of dextran, and phenylboronic acid (PBA) grafted onto the dextran as illustrated in Figure 1.

Previous research suggests that MNPs improve the stability of drugs through encapsulation, and prolong the desired therapeutic effects of encapsulated drugs by releasing them in a controlled manner over a period of five days [8]. This platform, however, is only suitable for encapsulation and delivery of hydrophobic drugs such as Cyclosporine A (CsA) and used to treat dry-eye disease. If this is to be implemented to treat adenoviral conjunctivitis, it must adapt to a hydrophilic system since most of the current treatments involve hydrophilic compounds.

This thesis aims to manipulate the MNP platform to generate a drug delivery system capable of enhancing hydrophilic drug efficacy of topical formulations targeting anterior segments of the eye. A double emulsion polymeric MNP (DE MNP) was developed as the ocular drug delivery platform to

encapsulate hydrophilic drugs in the core of the NPs, while maintaining mucoadhesive functionality in the shell of the NP.

The surfaces of these DE MNPs exhibited phenylboronic acid (PBA) moieties, which can covalently target the sialic acid moieties that are abundant on the ocular mucous membrane. These DE MNPs were evaluated for size and morphology. Fluorescein isothiocyanate dextran (FITC-Dex), a commercially used fluorescent dye, was used as a model drug to determine the capability of DE MNPs to encapsulate and release hydrophilic molecules. Povidone-Iodine (PVP-I), a commercially available drug commonly used to treat adenoviral conjunctivitis, was encapsulated and evaluated for bactericidal activity upon release from DE MNPs. Finally, animal studies were used to evaluate the mucoadhesive properties of DE MNPs and calculate their ocular retention time.

1.2 Research objectives

The overall objective of the proposed project is to evolve an established mucoadhesive nanoparticle drug delivery system developed by the Frank Gu Research Group, capable of enhancing therapeutic efficacy of hydrophobic topical formulations targeting anterior segments of the eye, to include hydrophilic drug molecules. We hypothesize that double emulsion mucoadhesive NPs would enhance topical delivery of hydrophilic drugs by improving their specific targeting and prolonged retention in the eye. By providing controlled drug release, DE MNPs would improve the bioavailability of hydrophilic drugs in the eye, requiring reduced frequency of administration and resulting in improved therapeutic efficacy. The specific objectives of the study are as follows:

1. Establish biodegradable polymers that are commonly used to prepare water-in-oil-in-water (W/O/W) double emulsions capable of encapsulating and controlling the release of therapeutics.
2. Synthesize double emulsion nanoparticles, through use of biodegradable polymers and PLA-Dex-PBA
3. Characterize the size, morphology, drug encapsulation, and drug delivery capacity of the nanoparticles formed using FITC-Dex as a model drug
    a. Demonstrate mucoadhesion properties of DE MNPs
    b. Demonstrate the prolonged ocular retention of DE MNPs on the ocular surface of rabbits
4. Test the application of DE MNPs for topical ocular delivery using PVP-I
    a. Demonstrate efficacy of therapeutic dose against bacteria

1.3 Thesis outline

This thesis is comprised of 6 chapters: the introduction, a literature review, three experimental research-based chapters, and a final chapter featuring the conclusion and recommended future work.

Chapter 1 introduces the key challenges that will addressed in the thesis, the hypothesis and research objectives to test this hypothesis.

Chapter 2 reviews the current status of using nanoparticles for hydrophilic drug delivery using biodegradable polymers.

Chapter 3 describes the methods behind the synthesis of DE MNPs, and the *in vitro* and *in vivo* characterization of the nanoparticles formed from the solvent evaporation process. This chapter focuses on the efficacy of DE MNPs as hydrophilic drug carriers using a using a fluorescent dye (FITC-Dex) as the model drug.

Chapter 4 presents the methods of evaluating the mucoadhesive capabilities of DE MNPs both *in vitro* and *in vivo*. This chapter focuses on the specific targeting of DE MNPs to sialic acid on the mucus membrane of the anterior surface of the eye and the ability of DE MNPs to prolong retention of hydrophilic drug carriers, using a fluorescent dye (FITC-Dex) as the model drug.

Chapter 5 describes the methods of determining the feasibility of DE MNPs to encapsulate hydrophilic antimicrobial agents and exhibit bactericidal activity *in vitro* when released from DE MNPs. This chapter focuses on the efficacy of DE MNPs as hydrophilic drug carriers using a using polyvinylpyrrolidone-iodine (PVP-I) as the antimicrobial drug.

Chapter 6 highlights the conclusions drawn from the research described in chapters 3, 4, and 5, and recommendations for future work based on these conclusions.

Chapter 2
Literature Review

2.1 Introduction: Hydrophilic Ocular Drug Delivery

Ocular drug delivery remains among the most challenging approaches to administering therapeutic agents because a successful therapeutic treatment requires circumventing both anatomical and physiological barriers in order to preserve the therapeutic drug concentration at the target site. These barriers come in the form of physiochemical limitations of the biopharmaceuticals themselves, the physiology and anatomy of the anterior and posterior segments of the eye, and the formulation conditions of the carriers for therapeutic agents. Furthermore, many drugs need to pass through one or more cell membranes to reach their site of action [9]. This is not a problem for small hydrophobic drugs, however for larger hydrophilic drugs, penetrating biological membranes is challenging, resulting in reduced therapeutic efficacy due to low permeability and bioavailability [10].

The main routes of administration of biopharmaceuticals include topical, periocular, suprachoroidal, and intravitreal. Topical administration in the form of ophthalmic drops is the most popular and preferred route to treat anterior segment diseases due to its non- invasiveness and ease of application. However, it is very difficult to achieve therapeutic drug concentrations by this method because of precorneal factors such as blinking, nasolacrimal drainage, and transient residence time in the cul- de-sac [1]. Furthermore, the lipoidal nature of the corneal epithelium restricts the entry of hydrophilic drug molecules and as a result, topically applied drugs have an ocular bioavailability of less than 5% [11]. For these reasons, there is a need to develop novel ophthalmic biopharmaceutical drugs and delivery systems, ideally targeting these macromolecules to biologically relevant ocular tissues [1].

In order to overcome these barriers and to increase contact time of drugs on the surface of the eye, several technologies have been developed for the delivery of drugs to our systems like liposomes, hydrogels, microparticles, micelles, implants...etc. There is no one technology that is suitable for any drug to any site, however biodegradable colloidal systems appear to be the most advantageous. Their popularity stems from their biocompatibility with ocular tissues, high encapsulation efficiency, sustained release, and ability to degrade into non-toxic by-products that are safely cleared from ocular tissues [12]. Natural and synthetic biodegradable polymers have been thoroughly explored and approved by the FDA for human applications in ocular delivery systems [11].

This review aims to examine the challenges surrounding successful hydrophilic drug delivery to ocular tissues, exploring various biodegradable drug delivery systems designed for human ophthalmic disease therapy.

2.2 Challenges in Hydrophilic Drug Delivery

2.2.1 Physiochemical Properties of Hydrophilic Drugs

Bioavailability of hydrophilic drugs depends largely on their ability to cross biological cell membranes as they possess intracellular target sites [13]. The lipophilic nature of biological membranes acts as a major barrier for hydrophilic drugs as it impedes their entry into cells. Additionally, the presence of tight junctions in the cornea, sclera, and retina, and the lipophilic nature of the corneal epithelium, hinders the permeation of these hydrophilic therapeutics [14]. Many of these large and hydrophilic drugs come in the form of protein and peptide pharmaceuticals which have gained a lot of popularity in the last decade due to their advantages over conventional small molecule drugs with respect to high potency, activity, low unspecific binding, less toxicity, and minimal drug-drug interaction [10]. Conventional molecules are typically low molecular weight, reasonably lipophilic and hence are quite stable and can be transported satisfactorily across cellular barriers into the blood and to their sites of action. They do not require sophisticated delivery systems unlike proteins which are unstable, high molecular weight, hydrophilic, complicated in structure, larger in size, and less permeable. As a result, they are harder to deliver by conventional ways. Additionally, the processes involved in the fabrication of drug delivery systems may inactivate the drugs in a number of ways including, but not limited to aggregation, denaturation, or chemical degradation [10]. Therefore, maintaining the structural integrity of hydrophilic drugs through all formulation steps of generating a delivery system is essential for its successful delivery. In addition, possible bioactivity loss and low stability of biopharmaceuticals due to interactions with the nanoparticle matrix, and extensive nanoencapsulation methods may further complicate the success of hydrophilic drug delivery.

2.2.2 Barriers due to Ocular Anatomy

The efficiency with which drugs are successfully delivered has largely been limited by the presence of ocular barriers. The human eye consists of two main components, the anterior surface which consists of the cornea, the conjunctiva, and the sclera [7], and the posterior surface which consists of the choroid and the retina, each of which have various biological barriers to protect the eye from foreign substances.

Upon the addition of biopharmaceuticals, there are several corneal factors and anatomical barriers that come into play and negatively affect the bioavailability of these formulations. Precorneal factors include solution drainage, blinking, tear film, tear turnover, and induced lacrimation [15]. The first point of resistance is the tear film. Tear film has a high turnover rate of 16%/min of the tear volume, as its function is to clear debris and pathogens from the ocular surface [16]. Human tear volume is estimated to be approximately 7-9µL, meanwhile the cul-de-sac can temporarily encompass around 30µL of an administered eye drop. The increase in the volume due to topical installation causes reflex blinking and rapid drainage from the ocular surface leading to a majority of the applied medication to be drained from the surface through the nasolacrimal duct within 15-30 seconds of installation [15]. Considering these precorneal factors, contact time with the adsorptive membranes of the ocular tissue is significantly lowered, resulting in less than 5% of the applied dose reaching the intraocular tissues [7].

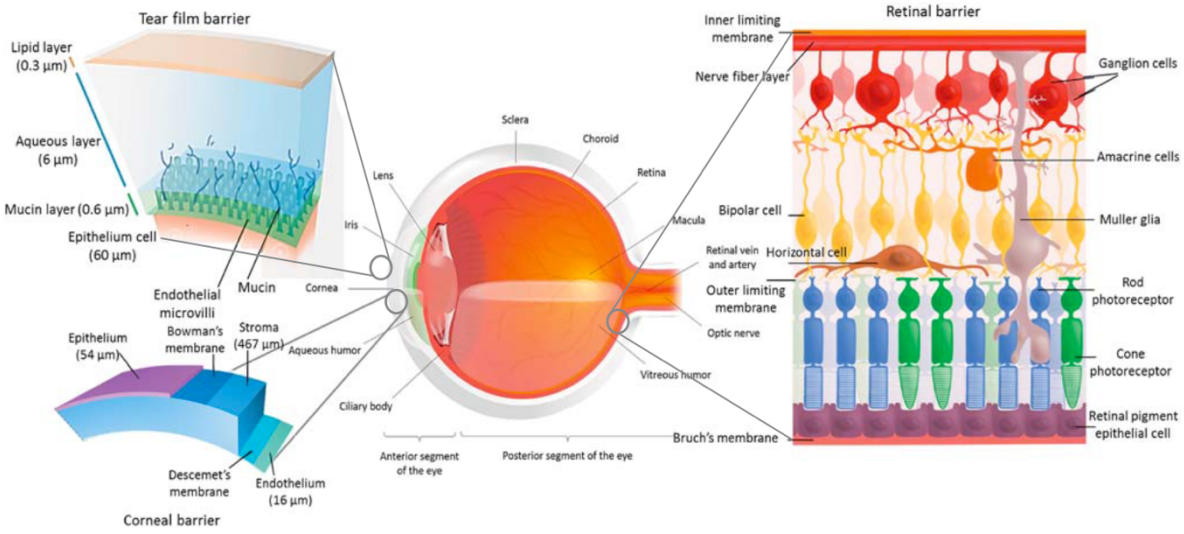

Figure 2.1 Ocular anatomy and tissue barriers. Reprinted from [1]**.**

The cornea, the anterior-most layer of the eye, acts as a mechanical barrier which limits the entry of foreign substances into the eye and protects the ocular tissues. It contains three main layers: the epithelium, stroma and endothelium. Each of these layers has a different polarity affecting the permeation of topically administered drugs. The corneal epithelium is lipoidal in nature which limits permeation of hydrophilic drug molecules. The stroma, unlike the epithelium, is highly hydrated and acts as a barrier to the permeation of hydrophobic drug molecules. The endothelium, the innermost layer to the cornea, separates the stroma from the aqueous humour and contains leaky junctions that facilitate the passage of biopharmaceuticals between the stroma and the aqueous humour [17]. Besides the

anatomical characteristics of the cornea that produce significant barriers to drug absorption, the presence of drug metabolizing enzymes, such as esterases, peptidases, and proteases, present in the corneal epithelium, the outer-most layer of the cornea, significantly impacting drug bioavailability [15].

The conjunctiva and the sclera play a critical role in the permeation of drugs that have poor corneal permeability. The conjunctiva contains tight junctions that are wider than those in the corneal epithelium, thus permitting hydrophilic molecules, however it is a highly vascular organ, thereby a significant source of drug loss into systemic circulation. The conjunctiva, similarly to the corneal epithelium, also contains drug metabolizing enzymes which limit drug bioavailability [18] .Finally, the sclera consists of collagen fibers and proteoglycans embedded in an extracellular matrix. The permeation of positively charged drugs is typically impacted as a result of binding to negatively charged proteoglycans [19].

Next, drugs are exposed the choroid, a network of blood vessels supplying the retinal pigment epithelium (RPE). The RPE acts as the major barrier that limits the entry of protein drugs from the choroidal blood circulation [20]. The charge and charge density of the drug itself also plays a role in determining its transport across the capillary endothelium [21]. The blood aqueous barrier (BAB) present in the posterior segment is divided into inner and outer blood retinal barrier (BRB). The inner BRB is composed of tight junctions between retinal capillary endothelial cells and is anatomically similar to the blood-brain barrier (BBB). The outer BRB is formed by the tight junctions between RPE cells. The high density of tight junctions and pericytes render the inner BRB highly effective in limiting transport of drugs from the blood into the retina [22].

To date, most common ophthalmic drugs are administered topically in the form of eye drops on the corneal surface. Alternative delivery methods such as intravitreal or periocular injections have been developed to improve the bioavailability of the therapeutic agents, but due to the invasive nature of these methods, side effects such as retinal detachment or intravitreal hemorrhage have been observed [23]. As a result, topical application in the form of ophthalmic drops has been the method of choice for administered pharmaceutical agents for the treatment of infection affecting the anterior segment. This route has been extensively utilized, but is limited by the narrow lachrymal capacity and constant tear drainage. The challenges affiliated with these conventional methods of ocular drug delivery have lead scientists to contribute significant effort into developing advanced drug delivery systems.

2.3 Advantages of Nanoparticles for Ocular Drug Delivery

At present, nanocarrier-based ocular drug delivery systems appear to be the most promising tool to meet the primary requirements of an ideal ocular delivery system. Nanocarriers, due to their small sizes, are likely to have high diffusivity across membranes such as the corneal epithelium: a significant number of studies have already demonstrated that the use of such nanomaterials via topical administration improved the corneal permeability of drugs [24], [25]. Similarly, due to their high surface-area-to-volume ratio, nanocarriers may also show improved interaction with the mucous membrane of the corneal surface to prolong the retention of the topically administered drug formulations.

Biodegradable polymers have been thoroughly investigated for sustained hydrophilic drug delivery. These polymers degrade into non-toxic monomer by-products that are safely cleared from the eye and systemic circulation. Polyesters such as Poly(lactic-co-glycolic acid) (PLGA) and Poly(lactic acid) (PLA) are among the most common biodegradable polymers constituting micro/nanospheres. Their popularity stems from their biocompatibility, high encapsulation efficiency, sustained release, and ability to degrade into non-toxic by-products that are safely cleared from ocular tissues [12]. Other constructive materials include polyanhydrides [26] and cyclodextrins [27].

Polymeric micelles

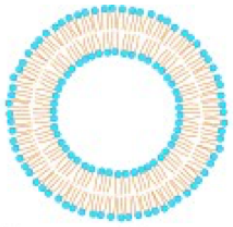

Liposomes/niosomes

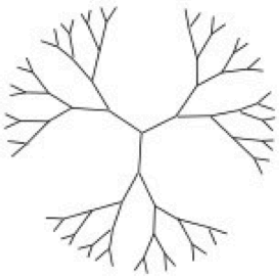

Dendrimer

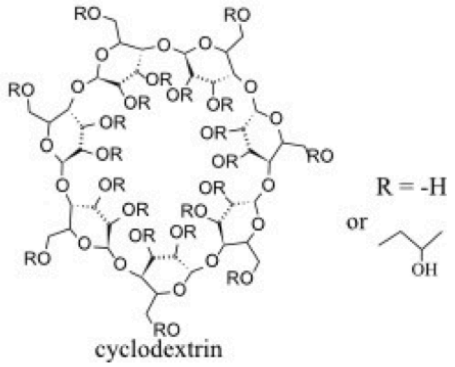

cyclodextrin

Figure 2.2 A schematic illustration of different nanomaterial-based ocular drug delivery systems. Reprinted and modified from [2]**.**

Nanoparticles are generally composed of biodegradable polymers and lipids and include microparticles, liposomes, dendrimers, micelles, and nanowafers that are actively used as carriers for targeted delivery of hydrophilic drugs. Drug release from nanoparticles is dependent on physiochemical factors such as the rate of degradation of polymers and molecular mass. The surface charge of the nanoparticles also plays a crucial role in ocular penetration. One study demonstrated higher diffusion of anionic human serum albumin based nanoparticles in the vitreous relative to cationic particles [28]. Such negatively charged nanoparticles may be utilized to deliver positively charged drug molecules.

Nanoparticles can be administered via various routes including topical, periocular, suprachoroidal and intravitreal. However, intravitreal injection often leads to clouding of the vitreous due to scattering of light by polymeric particles. While microparticles tend to sink to the lower part of the vitreal cavity attributed to their higher molecular mass. There are several examples of nanoparticle-mediated ocular delivery systems for small molecules at pre-clinical and clinical stages, however only few for high molecular weight hydrophilic drugs like proteins and peptides. These are at early stages of development as demonstrated by successful delivery of IgG using anionic gold nanoparticles to the photoreceptor cells and the RPE by subretinal injection [29]. Development of core-shell nanoparticles for encapsulating both hydrophobic and hydrophilic cargo [30], PEGylation for prolonging nanoparticle circulation and enhancing tissue penetration, functionalization for stimuli-responsive targeting and delivery of nanoparticles in biocompatible gels are some of the future strategies for controlled long-term delivery of biotherapeutics [31].

2.4 Recent Developments of Nanomaterials for Hydrophilic Drug Delivery

2.4.1 Microparticles

In order to encapsulate water soluble drugs, microparticles are successful when prepared using the double emulsion method. Single emulsion microparticles are limited in their ability for hydrophilic drug delivery due to hydrophilic drugs partitioning into the aqueous phase of the emulsion, producing a burst release of the drug upon administration [32]. The double emulsion method is a simple one that allows researchers to control process parameters to efficiently encapsulate water soluble compounds. Poly(lactic-co-glycolic acid) (PLGA) is the most widely used biomaterial for microencapsulation and prolonged delivery of therapeutic hydrophilic drugs. PLGA has excellent biodegradability and biocompatibility because its

degradation products, lactic acid and glycolic acid, are taken up by our body's citric acid cycle. The physicochemical properties of PLGA may be varied systematically by changing the ratio of lactic acid to glycolic acid which alters the release rate of microencapsulated therapeutic molecules. This is observed in a number of applications where PLGA microparticles prepared by the double emulsion method have shown varying release rates. In a study by Hachicha et al, the release of the vancomycin from PLGA microparticles in the first 24 h was around 90% [33]. Meanwhile, another study by Karal-Ylmaz et al. demonstrated the synthesis of PLGA microspheres for the controlled delivery of vascular endothelial growth factor, VEGF. They showed successful encapsulation and sustained release of biologically active VEGF molecules over a period of 28 days [34].

During microparticle formulation using conventional solvent evaporation methods, an emulsifier is required to ensure droplet stability until the polymer concentration in the organic solvent is high enough to maintain particle conformation. The most widely used emulsifier in the preparation of PLGA micro/nanoparticles is poly(vinyl alcohol) (PVA) [35]. Feng et al showed that D-α-tocopheryl polyethylene glycol 1000 succinate (vitamin E TPGS; FDA-approved as a water-soluble vitamin E nutritional supplement) markedly improved drug loading from 0.3 mg/ml to 5mg/mL when PVA as used [36].

The use of PLGA for drug delivery on the ocular surface carries unique challenges as the delivery of any therapeutic agent to the ocular surface will always be limited by tear clearance. Promising attempts have been made to overcome this hurdle with the development of mucoadhesive PLGA microparticles [37]. Chitosan, PEG, sodium alginate and poloxamers are examples of mucoadhesive polymers popularly used as a mucoadhesive coating in the formation of PLGA microparticles [38]. Chitosan-coated particles have shown mucoadhesion for up to 6 hours due to the positive surface charge which allows for their interaction with the negatively charged mucin chains on the ocular surface [37]. Though they offer many advantages, the obstacles hindering more widespread use of microparticle sustained-release formulations for clinical use include low drug loading, particularly of hydrophilic small molecules, high initial burst release and/or poor formulation stability [37].

2.4.2 Lipid-based Nanocarriers

Lipid-based nanoacarriers have been extensively used as a colloidal system for controlled ocular drug delivery. These include liposomes, solid lipid nanoparticles (SLNs) and nanostructured lipid carriers (NLCs). Liposomes are lipid bilayer structures formed by self-assembly of amphiphilic molecules [39]. They are advantageous as drug carriers due to their biocompatibility, minimal toxicity and antigenicity,

increased membrane permeability, and their ability to be metabolized *in vivo* [40]. The ability of liposomal systems to encapsulate both hydrophilic and lipophilic compounds enables a wide variety of drugs to be carried by these vesicles, including deoxyribonucleic acids (DNA), proteins, or imaging agents. When nucleic acids, molecules, or drugs are enclosed in a lipid-based coating, they have lower degradation rates than they would as free standing biopharmaceuticals because they are more readily taken up by cells via endocytosis [41]. The final organization, morphology, and physicochemical properties of lipid-based liposomes depends on the nature, size, and geometry of their lipid components, concentration, temperature, and surface charge [42].

Phospholipids are the most common amphiphile used for liposomal synthesis. Phospholipids are generally composed of one hydrophilic head and two hydrophobic tails. Depending on the composition of the phospholipids, liposomes can have positive, negative, or neutrally charged surfaces. When phospholipids are dispersed in water, they aggregate spontaneously into bilayers, which resemble the structures they form in biological membranes [42]. It has been concluded that cationic liposomes are more efficiently internalized by the corneal epithelium because they can interact more efficiently with negatively charged mucins at the ocular surface [43]. Generally, this positive charge of the liposomes has led to a greater corneal drug absorption by increasing drug residence time through ionic interactions [43], as well as an improved therapeutic effect [44]. In addition to the effect of the charge, the liposomal size has been reported to influence their interaction and transport across the cornea. Liposomes of sizes less than 100 nm generally exhibit significantly higher circulation times due to a decrease in opsonization of liposomes with blood serum proteins [45]. Though they offer many advantages, liposomes are typically unstable in biological media, and they are susceptible to phagocytic uptake and clearance. Encapsulation of biopharmaceuticals in liposomes is commonly achieved via a dehydration-rehydration method. Although this method yields high association efficiency without utilizing organic solvents and sonication (both factors that may cause drug denaturation), the high developmental cost and the instability of the particle size restricts its wide application.

Bevacizumab (Avastin), a synthetic monoclonal antibody against VEGF, has shown beneficial effects on treatment of AMD [46], myopic CNV [47], glaucoma [48], and DR [49]. However, it has a short intravitreal half-life (3-5 days) and several injections are needed to achieve a therapeutic effect [47]. To avoid complications of intravitreal hemorrhaging, retinal detachments and cataracts [48], and to increase the half-life of bevacizumab, Abrishami et al. encapsulated this protein into liposomes incorporated with cholesterol via the dehydration-rehydration method [50]. The results of this study showed prolonged residency of bevacizumab in the vitreous when encapsulated in liposomes in

comparison to free drug. Intravitreal injection of liposomes containing bevacizumab was well tolerated in rabbits through 42 days, providing a sufficient therapeutic concentration for neovascular eye diseases that was 5 times higher than free bevacizumab [50].

Solid lipid nanoparticles (SLN) are lipidic colloidal systems with an inner structure based on pure solid lipids. They are derived from oil-in-water (o/w) emulsions in which the liquid lipid is replaced with a solid lipid at room temperature. Several solid lipids such as stearic acid, triglycerides, carnauba wax, beeswax, cetyl alcohol, emulsifying wax, cholesterol butyrate, and cholesterol may be suitable for SLN preparation [1]. These solid lipids are typically biocompatible and offer various advantages including avoidance of organic solvents for formulation, improved physical stability and targetability, controlled release and easy scale-up [51]. However, low drug loading, burst-effect and rapid elimination by mononuclear phagocytic system (MPS) are some of the drawbacks of SLNs [52]. Due to their hydrophilic nature, most proteins are poorly encapsulated into the hydrophobic matrix of SLNs [53]. Some peptides such as cyclosporine A (CsA) are sufficiently hydrophobic to be encapsulated in the lipid core of SLNs. SLNs can be formulated by several methods such as high-pressure homogenization (hot and cold homogenization) [54], solvent injection [55], water in oil in water double emulsion (W/O/W) [56], high-shear homogenization [57], solvent emulsification evaporation and membrane contactor. W/O/W emulsions enhance the solubility of hydrophilic pharmaceuticals, allowing for delivery of hydrophilic macromolecules via SLNs [58]. Many studies evidenced that positively charged colloidal particles increase the penetration of drugs through mucosal barriers [59]. Chitosan (CS) is a cationic polysaccharide characterized by good mucoadhesive properties, penetration enhancement properties across various mucus epithelia and enzyme-inhibiting properties towards various proteolytic enzymes. Because the cornea and conjunctiva possess a negative charge [60], the administration of cationic particles has a positive impact on drug bioavailability. This is demonstrated by Bacsaran et al. who were able to incorporate CsA, commonly used to treat chronic dry eye syndrome, into cationic SLNs and improve the ocular penetration in both aqueous and vitreous humour [61].

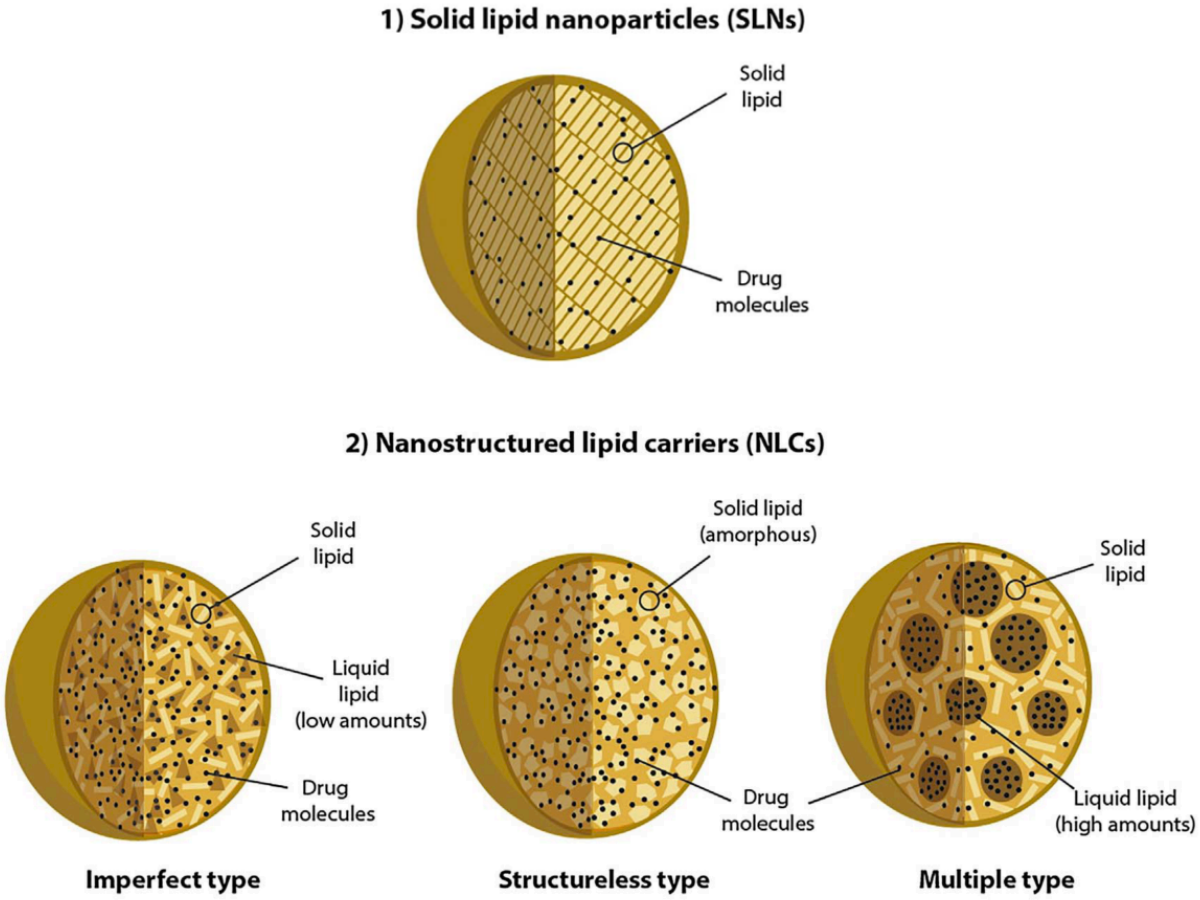

Figure 2.3 Schematic representation of solid lipid nanoparticles (1) and nanostructured lipid nanocarriers (2) used in drug delivery. Imperfect NLCs are prepared by mixing solid lipids with small amounts of liquid lipids (oils) to prevent crystallization. Structureless NLCs' lipid matrix is formed by a solid lipid that has an amorphous structure after solidification. Multiple NLCs are prepared using high amounts of liquid lipids blended with solid lipids. Reprinted and modified from [3]**.**

Solid lipid nanoparticles have several advantages over other types of nanoparticulate systems as discussed earlier in this section. However, there are some limitations too, the most challenging being the degradation of active components during the production process which may be attributed to the stress and strain associated with the homogenization process. Biopharmaceuticals are sensitive to both physical and chemical stresses, and need gentle handling. The production of heat during processing may also cause drug degradation so the selection of a proper production method is vital [15].

NLCs were developed to overcome the limited drug loading associated with modifications and higher

water content of aqueous SLN dispersions. NLCs are composed of highly disordered solid and liquid lipids and can provide better drug protection and entrapment efficiency in comparison to SLNs [62], [63]. Shen et al. investigated the potentiality of CsA-loaded thiolated NLC as mucoadhesive delivery systems for topical ocular administration [64] and found that the addition of cysteine–polyethylene glycol stearate (a thiolated PEG derivative, which acts as a nonionic surfactant) on the NLC surface extended the precorneal retention time of the nanocarriers and improved the biodistribution of CsA in the conjunctiva. This achieving a satisfactory drug concentration within 24 h for an efficient immunomodulation [64]. Both SLNs and NLCs have shown potential in delivering small molecules to ocular tissues [39]. Conversely, efficiency in delivering hydrophilic protein and peptide-based biopharmaceuticals to ocular tissues has not been fully exploited and requires further investigation.

2.4.3 Dendrimers

Dendrimers are monodisperse macromolecules that constitute branched, layered architectures composed of synthetic polymers that show promise as nanocarriers in several biomedical applications [4]. Some of the commonly used dendrimers are based on polyamidoamines, polyamines, polyamides (polypeptides), poly(aryl ethers), polyesters, carbohydrates and DNA. Among these, polyamidoamine (PAMAM) based dendrimers are most commonly used and commercially available. Unlike linear polymers, the multivalent property of dendrimers provides a means to achieve high concentrations of payloads including small-molecules, biopharmaceuticals and imaging agents [65].

The molecular weight and surface charge of dendrimers also play a crucial role in determining tissue accumulation profiles, drug release rates (from the polymer) and elimination rates. While, high molecular weights of dendrimers (N 40 kDa) prevent rapid clearance, uncharged or negatively charged surface limit nonspecific interactions [65]. In addition, numerous end groups offer a way to precisely control functionality with multiple copies of drugs, chromophores, peptides, proteins and multivalent ligand density. Such surface modifications can not only strengthen ligand-receptor binding and improve the targeting of attached components but can also accelerate dendrimers stimuli-responsive activity [66].

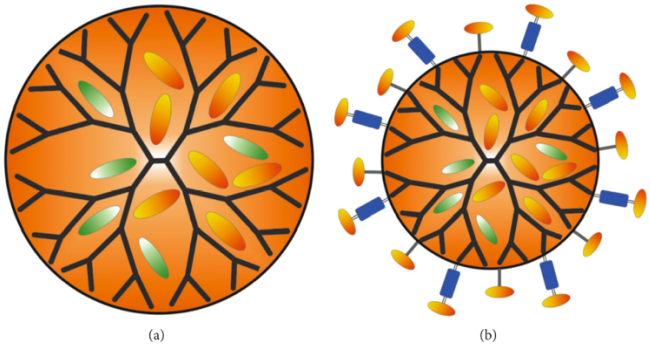

Figure 2.4 Schematic representation of drug encapsulated (a) and drug conjugated (b) dendrimers. Reprinted from [4]**.**

PAMAM dendrimers as drug delivery vehicles for small molecules have shown improved biological response, tolerability and lower clearance from the ocular surface indicating their utility as an eye drop formulation [67]. PAMAM dendrimers showed remarkable interactions with membrane-associated mucin layers [67]. This is important because interactions between the nanoparticulate surface and tear film is one of the key factors for corneal permeation and increased residence time [66]. pH-dependent interactions of PAMAM dendrimers with ocular mucins were also investigated, suggesting stronger interactions at pathological conditions (pH 5.5 for tear fluid) compared to physiological conditions. A larger fraction of primary amine surface groups of PAMAM-NH_2 dendrimers are protonated at low pH, resulting in a net-positive charge leading to an increased association with mucins. Research findings by Yao et al. reported increased permeation and retention time of cationic PAMAM dendrimer-puerarin complexes with increased bioavailability of puerarin in aqueous humor, further supporting the above data [68]. Other studies have also confirmed the delivery of biopharmaceuticals using different conjugation techniques with dendrimers. Tarallo et al. report the synthesis of a poly(amide)-based dendrimer functionalized at the termini with a membrane-interacting peptide derived from the herpes simplex virus (HSV) type 1 glycoprotein H (gH625–644). The peptidodendrimer inhibits both HSV-1 and HSV-2 at a very early stage of the entry process, preventing the virus from coming into close contact with cellular membranes, showing promising inhibitory activity towards viruses of the Herpesviridae family [69].

2.4.4 Polymeric Micelles

Polymeric micelles represent a class of nanocarriers that are composed of amphiphilic polymers which self-assemble in aqueous media to form organized supramolecular structures. Most of the polymeric micelles used in drug delivery consist of amphiphilic di-block (hydrophilic-hydrophobic) polymers, tri-

block (hydrophilic-hydrophobic- hydrophilic) polymers, graft (hydrophilic-hydrophobic) and ionic (hydrophilic-ionic) copolymers such as Pluronics, polyesters, and poly(L-amino acids). For the majority of these systems, poly(ethylene glycol) (PEG) is the primary hydrophilic segment [70]. Micellar formation confides upon the reduction of the interfacial free energy [71]. The degree of self-aggregation generally depends on the polymer chain concentration, the properties of the drug or any targeting agents, and the mass and composition of the copolymer backbone [72]. Depending upon the molecular weight of the block copolymers, micelles can have different shapes including spherical, cylindrical and star-shaped structures [73]. Pepić et al. developed Pluronic F127 (F127) and CS cationic polyelectrolyte based micelles for dexamethasone (DEX). *In vivo* biodistribution studies in rabbits revealed an increase in bioavailability of DEX (AUC162.8 ± 11.23) in comparisons to commercial DEX (0.1% w/v eye drop (AUC67.5 ± 9.42) and F127 alone (AUC115.9 ± 8.31) which is attributed to the synergistic enhancement of transcorneal permeation caused by F127 and CH [74]. Liu et al. synthesized polymeric micelles using block-copolymer PLA-Dex surface functionalized with phenylboronic acid (PBA) for ocular delivery of CsA to treat dry-eye disease. PBA's hydroxyl groups bind to SA through covalent diol-diol binding, allowing these polymeric micelles to stay on the mucus membrane and deliver drugs effectively over a longer period of time than commercial options [8]. The PBA modified NPs demonstrated encapsulation of Cyclosporine A (CsA), a dry eye treatment drug, and sustained release for up to 5 days *in vitro*, showing their potential as a long-term eye drop delivery platform. Gadad et al. prepared moxifloxacin loaded PLGA nanosuspensions, with entrapment efficiency up to 83.1%. These particles showed significantly higher permeation capability compared to commercially marketed eyedrops in ex vivo transcorneal permeation studies and also showed better antimicrobial efficacy compared to the marketed formulation [75].

Polymeric micelles possess high biocompatibility, biodegradability, and multiplicity of functional groups. Their hydrophilic shell limits opsonin adsorption, which contributes towards a longer blood circulation time and evasion of scavenging by the MPS system. Nonetheless, they also suffer from low cellular uptake and tissue accumulation, instability upon dilution and limitations in entrapping hydrophilic drugs [1].

2.4.5 Nanowafers

Nanowafers are tiny transparent circular discs that are composed of various polymers including poly(vinyl alcohol) (PVA), polyvinylpyrrolidone (PVP), (hydroxypropyl)methyl cellulose (HPMC), and

carboxymethyl cellulose (CMC). These are generally applied with a fingertip on the ocular surface and can withstand constant blinking without being displaced unlike topical eye drops. Nanowafers consist of arrays of drug-loaded nanoreservoirs which release drugs in a highly controlled manner ranging from a few hours to several days. The synergistic action between the polymers and the loaded drug leads to slow drug release thus enhancing drug residence time and subsequent absorption into ocular tissues [1].

Yuan and group demonstrated the sustained release and enhanced corneal permeability of doxycycline-loaded PVA nanowafer over 24 h in mice [76]. The same group reported the efficacy of such PVA fabricated nanowafer loaded with axitinib for treating CNV in a murine ocular burn model demonstrating that once a day axitinib delivery by nanowafers was more efficacious than the twice a day topical eye drop treatment [76]. Importantly, at the end of stipulated drug release time, the nanowafer dissolves and fades away thus rendering ocular surfaces free of polymers [1].

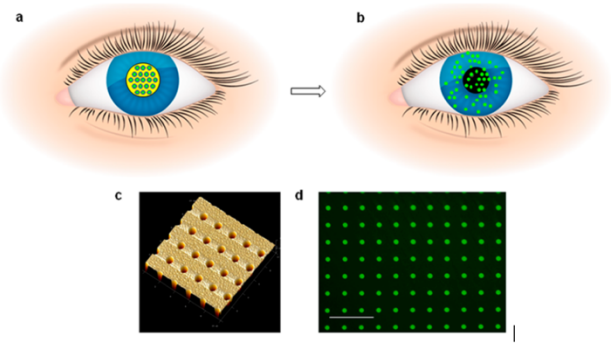

Figure 2.5 Ocular drug delivery nanowafer: (A) Schematic of nanowafer instilled on the cornea. (B) Diffusion of drug molecules into the corneal tissue. (C) Nanowafer on a fingertip. (D)AFM image of a nanowafer demonstrating an array of 500nm diameter nanoreservoirs. Reprinted and modified from [1].

2.5 Conclusions/Future Perspectives

The field hydrophilic ocular drug delivery has taken a significant stride forward with the advent of nanotechnology. Numerous recent studies have focused on using various types of natural or synthetic biodegradable polymers, such as chitosan, hyaluronic acid, PVP, PEO, PLA, PGA, PLGA and etc., as building blocks for nanomaterials making them biocompatible and non-toxic. Popular nanomaterials for hydrophilic drug delivery, such as microparticles, lipid-based nanoparticles, dendrimers, polymeric micelles, and nanowafers as drug carriers, were proven to increase the ocular bioavailability of various therapeutic agents. Topical administration of the drugs associated with these nanomaterials showed

sustained release of hydrophilic biopharmaceuticals which increased the duration of therapeutic activity, consequently reducing the need for frequent administration. Furthermore, these formulations did not affect the integrity or functionality of these therapeutics upon encapsulation. In the last decade, a great deal of research has focused on the controlled delivery of large hydrophilic compounds, such as protein and peptide drugs for various ocular indications like age related macular degeneration (AMD), choroidal neurovascularization (CNV), dry eye (DE), glaucoma, cataracts, and diabetic retinopathy (DR).

Chapter 3
Development of Double Emulsion Mucoadhesive Nanoparticles for Topical Ocular Drug Delivery

3.1 Summary

Mucoadhesive NP drug carriers have attracted substantial interest as a potential solution to the low bioavailability of topical formulations. In this study, NPs composed of a PLGA core and PLA-Dex-PBA shell were developed as mucoadhesive NP drug carriers (DE MNPs). The DE MNPs encapsulated up to 85 wt% and exhibited sustained drug release for up to 7 days *in vitro*. Furthermore, DE MNPs show increase in DL% with increase initial wt%, but decrease in DL% with increase in MWt. These data show that DE MNPs have the potential for being a promising new ocular delivery system capable of encapsulating hydrophilic compounds and can be tuned to improve drug loading and release.

3.2 Introduction

Poly(lactic-co-glycolic acid) (PLGA), a biodegradable and biocompatible polymer, has the ability to degrade into non-toxic by-products (lactic acid and glycolic acid) that are metabolized by the human body. Encapsulation of drugs in PLGA based nanoparticles are popular because of the relatively slow rate of release of drugs over a prolonged period of time, allowing for less frequent administrations [77]. This is ideal because it increases patient compliance, reduces the discomfort of frequent administration to the eye, protects the therapeutic compound on the surface of the eye, and avoids peak-related side-effects [78].

So far, several formulations have been investigated to encapsulate hydrophilic drug substances, such as proteins and peptides, into a PLGA matrix using W/O/W double emulsion method. However, achieving functionalities such as passive targeting and active targeting using PLGA-based drug delivery systems is difficult because there is a deficiency of functional groups on the PLGA surface [77]. The conventional PLGA surface makes it challenging to achieve the cell affinity and immobilization of cell-targeting molecules. Therefore, modifying the surface of a PLGA-based drug delivery system is essential especially in organs such as the eye where targeted drug delivery is important to the efficiency of the drug being delivered.

PLGA polymer chains and repeating units are mainly composed of ester groups whose activity is very low and hard to react with other functional groups. Although the uncapped PLGA with free carboxyl

(COOH) termini was widely adopted, no obvious improvement in PLGA activity performance has been found [79]. Bifunctional poly(ethylene glycol) (PEG) (amine group (NH_2)-PEG-NH_2, MW of PEG 3–5 kDa) has also been used as bio-linker between PLGA and active targeting molecule [80], involving multistep reactions. However, there is limited functional groups for the targeting molecule to attach on as one PLGA polymer chain can only get one reactive NH_2 from the bio-linker bifunctional PEG. This greatly affects the properties of the PLGA surface and its reaction with other targeting molecules [77].

The objective of this study was not to modify the surface of PLGA itself, but rather to modify the double emulsion method such that the second emulsion contained mucoadhesive properties. The double emulsion method was chosen because it retains the hydrophilic shell necessary for compatibility with the physiological environment in the eye at the surface, and also allows for encapsulation of hydrophilic compounds in the core. The first step in the double emulsion method consists of generating the first emulsion, a water-in-oil (W/O) emulsion, where the aqueous solution contains the hydrophilic active component, and the organic phase contains a polymer, such as PLGA, and a suitable surfactant with a low hydrophile-lipophile balance (HLB) typically between 4 and 6, such as SPAN80. The first emulsion is formed under high speed homogenization. The second emulsion, a water-in-oil-in-water (W/O/W) emulsion, typically consists of a hydrophilic surfactant with a higher HLB, typically between 8 and 18, in a larger aqueous volume that is also exerted under shear stress [81]. Here, PLGA and SPAN80 were used to generate the first emulsion, and PLA-Dex-PBA was used as the surfactant with a higher HLB (10.5) than SPAN80 (4.3) in the second emulsion.

The main drawbacks of the double emulsion method are the large sizes of the NPs, which have been documented to stimulate reflex tearing, and cause irritation and discomfort [82], and the leakage of the hydrophilic active components, responsible for low entrapment efficiencies [83]. Here, we consider polymer and surfactant ratios, polymer concentration, and polymer molecular weight based on previous work [84], [78], [85], [86] to generate a double emulsion mucoadhesive drug delivery carrier that is small in size and has high entrapment efficiencies of hydrophilic compounds.

3.3 Experimental Section

3.3.1 Materials

Fluorescein-isothiocyanate dextran (MW 3kDa, 10 kDa, 40kDa), Poly(D,L – lactide-co-glycolide) (MW 45 kDa – 75 kDa), SPAN80®, Dimethyl sulfoxide (DMSO), Dichloromethane (DCM), Dextran (MW: 10 kDa), 3-Aminophenylboronic acid monohydrate (PBA), sodium periodate ($NaIO_4$), glycerol, sodium cyanoborohydride (NaCNBH3), N-acetylneuraminic acid (SA) were purchased from Sigma Aldrich

(Canada). Acid-terminated PLA (MW: 20 kDa) was purchased from Lakeshore Biomaterials (USA) and washed with methanol to remove monomer impurities. TEM grids (F/C 400 mesh Cu) were purchased from Ted Pella (USA). Phosphotungstic acid was purchased from Fisher (Canada); uranyl acetate and lead citrate were borrowed. Simulated tear fluid (STF) was generated for the *in vitro* drug release experiments using a previously documented formulation [64].

3.3.2 Synthesis

Synthesis of a water-in-oil-in-water (W/O/W) emulsion first involved the formation of the primary emulsion (W/O). The primary emulsion was made by dissolving FITC-Dex (at desired concentration) in 0.4mL of MilliQ and adding that to 2mL of 10mg/mL PLGA dissolved in DCM containing 5% w/v SPAN80. DCM and MilliQ are immiscible liquids that require ultrasonification to homogenize. Using the Fischer Scientific Branson Probe Sonicator, the mixture was sonicated for 30 seconds (pulse 0.2, amplitude 30) to obtain a primary water-in-oil emulsion [83].

The primary emulsion was then added to a larger aqueous phase containing a surfactant in order to produce the secondary emulsion (W/O/W). The surfactant used in this phase was the amphiphilic block copolymer PLA-Dex-PBA which was prepared using a previously reported method [106]. In brief, PLA-Dex-PBA was synthesized by dissolving PLA-Dex in DMSO (30 mg/ml), and added slowly into water under mild stirring. Oxidation of the dextran surface was carried out by adding 60mg of sodium periodate ($NaIO_4$) and stirring for an hour. Subsequently, glycerol was added to quench the unreacted $NaIO_4$. Surface functionalization with PBA was carried out using reductive amination in the presence of $NaBH_3CN$ for 24 hours. The mixture was then dialyzed in H_2O for 24 hr to remove any unreacted solutes, changing the wash medium 4 times. All reactions were carried out in dark [106].

To generate the second emulsion, PLA-Dex-PBA was dissolved in DMSO (12.5mg/mL) and added dropwise to 12.5 mL of MilliQ under vortex to generate a 0.1% w/v PLA-Dex-PBA solution. The primary emulsion was then immediately added to the 0.1% w/v PLA-Dex-PBA solution and homogenized using the Fischer Scientific Branson Probe Sonicator for 30 seconds (pulse 0.2, amplitude 30) to obtain a water-in-oil-in-water emulsion. The mixture was left to evaporate the organic solvent overnight while under stirring (490rpm) then dialyzed in 1L of DI H_2O the next morning using 12-14K molecular weight cut-off (MWCO) dialysis tubing for 1.5 hours to remove the DMSO. To make blank DE MNPs, the same process was followed, however 0.4mL of MilliQ was used to generate the first emulsion.

3.3.3 Characterization of PLA-Dex-PBA DE MNPs

The mean particle diameter and polydispersity index (PDI) was determined using Dynamic Light Scattering (DLS) by measuring the Multimode-Size Distribution (MSD) volume-averaged mean diameters using a 90Plus Particle size Analyzer (Brookhaven, λ = 636 nm at 90°). The analysis was performed at room temperature, at a scattering angle of 90ºC. DE MNPs were filtered through a syringe filter (pore size = 200nm) to remove the drug and NP aggregates, then diluted 20x prior to analysis. The zeta potential of the Control (no drug) DE MNP and the drug containing (encapsulated) DE MNP were measured using Zetasizer Nano ZS (Malvern Instruments Worcestershire, U.K.) using 200nm filtered sample. The sizes and morphology were further analyzed by Static Light Scattering (SLS). SLS measurements were processed in batch mode using a multi angle laser light scattering apparatus (Brookhaven BI-200SM Laser Light Scattering System) equipped with a 25mW Ga/As laser beam operating at λ = 636 nm. Light scattering intensities recorded at 5 angles between 45º and 155º were derived with the ASTRA software according to the Zimm procedure. The sensitivity of the SLS is greater than the DLS, thus the DE MNPs were further diluted 50x prior to analysis. Measurements of hydrodynamic radius (R_h) and radius of gyration (R_g) were obtained and used to assess DE MNP conformation. These findings were also confirmed using Transmission Electron Microscopy (TEM) equipment by drying the DE MNP suspension on 300 Mesh Formvar coated copper grids (Canemco and Marivac) and using phosphotungstic acid solution as the negative stain. TEM findings were further explored using a double staining method by drying the DE MNP suspension on 300 Mesh Formvar coated copper grids (Canemco and Marivac) and using lead citrate followed by uranyl acetate to stain the particles.

3.3.4 FITC-Dex encapsulation

The encapsulation of FITC-Dex in the DE MNPs was accomplished by dissolving the hydrophilic (model) drug in MilliQ for the aqueous phase in the primary emulsion. The DE MNPs, post dialysis, were filtered through a syringe filter (pore size 200nm) to remove the drug and NP aggregates. The NPs were subsequently filtered through Amicon filtration tubes (MWCO = 30 kDa, Millipore for 3kDa and 10kDa FITC-Dex loaded DE MNPs, MWCO = 100 kDa, Millipore for 40kDa FITC-Dex loaded DE MNPs) to further remove any remaining free drugs in the suspension. The filtered DE MNPs containing encapsulated FITC-Dex were re-suspended and diluted in DMSO. The drug loading (wt%) in the polymer matrix was calculated by measuring the concentration of FITC-Dex in the solution by obtaining the absorbance at 518nm using Epoch Multi-

Volume Spectrophotometer System (Biotek). The measurements were obtained in triplicate (n=3, mean ± S.D). The absorbance measured by the same procedure using DE MNPs without encapsulated drug was used as the baseline. The absorbance was correlated using a standard calibration curve of FITC-Dex in DMSO. The encapsulation efficiency (%) and drug loading (wt%) were calculated using the two equations below.

$$\mathrm{EE\%} = \frac{[\mathrm{Drug}]_{\mathrm{actual}}}{[\mathrm{Drug}]_{\mathrm{theoretical}}} \times 100\%$$

Equation 1. Encapsulation efficiency

$$\mathrm{DL\%} = \mathrm{EE} \times \mathrm{DL\%}_{\mathrm{theoretical}}$$

Equation 2. Drug Loading

3.3.5 *In vitro* release

Drug encapsulated NPs were prepared and filtered (pore size: 200nm) to remove non-encapsulated drug aggregates. A purified sample of NP-drug suspension was collected to measure the maximum absorbance and this was used as the 100% release point. Subsequently, 4mL of the NP-drug suspension was transferred to a dialysis membrane (MWCO = 100 kDa, Fisher Scientific) and dialyzed against 150 mL of simulated tear fluid (STF, pH 7.4) at 37 °C under mild stirring. At predetermined time intervals, 1 mL of the release medium was extracted and the same volume of fresh new STF was added to the release medium. The extracted release medium was used to perform UV-Vis absorption measurements at 492 nm in triplicates (n = 3, mean ± S.E). The release medium was replaced at each time interval to maintain the concentration of FITC-Dex in the medium and to stay below the solubility limit of the FITC-Dex in STF. The release of free FITC-Dex was also obtained with identical procedure for comparative analysis. All experiments were performed in dark environment, and the beakers were sealed with Parafilm to prevent evaporation of PBS.

3.4 Results & Discussion

3.4.1 Size & Morphological Characterization

Double emulsions are thermodynamically unstable but may become kinetically stable depending on their formulation and processing. Coalescence and Ostwald ripening are two important mechanisms that destabilize double emulsion droplets, and the diffusion through the organic phase of the hydrophilic active component is the main mechanism responsible for low levels of entrapped compound [83]. The Ostwald

ripening process is generally modelled by the well-known Lifshitz-Slyozov-Wagner (LSW) theory, for O/W emulsions without excess of surfactant. This theory is based on the assumption that the diffusion of oil through water determines the overall Ostwald ripening rate of diffusion which may be accelerated by solubilization of oil in the aqueous phase [87]. Conversely, coalescence involves a diffusive transfer of the dispersed phase from smaller to larger droplets, causing fusion of droplets as a result of rupture of the thin film [87]. These factors can be overcome and the leakage effect reduced by using a high emulsifier concentration and a high polymer molecular weight. This would in turn increase the viscosity of the inner water phase.

Taking these limitations into consideration, we designed the DE MNPs to use high molecular weight PLGA (40-75kDa), and a high concentration of SPAN80 (5% w/v). SPAN80 was chosen because of its low HLB value and non-ionic nature, therefore improving solubilization characteristics such as non-irritancy, and ability to prolong precorneal retention with enhanced permeability [88]. The concentration of 5% w/v was determined empirically as the minimum concentration of emulsifier required to prevent phase separation immediately after sonication to produce the first emulsion.

Upon formation of DE MNPs using the solvent evaporation double emulsion method, their sizes and morphologies were characterized using light scattering techniques (DLS, SLS), and TEM respectively. FITC-Dex was used as the model drug to test the feasibility of DE MNPs a drug delivery system. Dynamic light scattering (DLS) was used to analyze the fluctuations in the intensity of scattering by droplets/particles due to Brownian motion [89]. Nanoemulsion droplet size, polydispersity, conformational shape and zeta potential were assessed using a particle size analyzer. These results are reported in Table 3.1.

Formulation	**Diameter[a)] (nm)**	**Mean PDI[b)]**	**R_g/R_h[c)]**	**ξ Potential[(d)] (mV)**
Blank DE MNPs	167 ± 1	0.0583 ± 0.0301	1.01 ± 0.05	-58.5 ± 2.1
FITC-Dex (10KDa;100wt%)	161 ± 2	0.0747 ± 0.0252	1.19 ± 0.05	-61.3 ± 1.4
Blank DE MNPs using PLA-Dex (n = 1)	155	0.0937	0.970	-43.8

Table 3.1 Characterization of blank and FITC-Dex loaded DE MNPs by (a) size, (b) polydispersity index, (c) conformation, and (d) surface charge; n = 3 ± s.e.

The sizes of DE MNPs were smaller than what was typically observed for double emulsions using PLGA in literature [85], [86], [90]. Small particle size is preferred for ocular drug delivery since larger particles have been documented to stimulate reflex tearing, and cause irritation and discomfort [82]. The sizes of blank DE MNPs (no drug) were comparable to those of FITC-Dex loaded (100wt%) DE MNPs ($P > 0.05$). Typically, the sizes of double emulsions are influenced by the polymer concentration [85], which were not significantly different (10KDa) between the control and FITC-Dex loaded samples. The small size produced by the double emulsion technique could be influenced by the stability of the primary emulsion. The more stable the primary emulsion, the smaller the particles [87].

The polydispersity index (PDI) of DE MNPs describes the degree of homogeneity of the NP distribution [89]. Since laser diffraction was used for this analysis, a rough equivalent of particle polydispersity could be given by two factors/values namely, uniformity (how symmetrical the distribution is around the median point) and span (the width of the distribution) [89]. Both samples gave a polydispersity index below 0.10, indicating that the distribution consisted of a single size mode without any aggregates. This was aided by filtering DE MNPs with a 0.2um sized filter which eliminated any aggregates and ensured the solution consisted of a homogenous population of DE MNPs. We expected to see two distributions, one double emulsion, and one micelle because of the amphiphilic nature of PLA-Dex-PBA. This was not evident in the PDI because the cumulant analysis can only determine the particle size distribution of a Gaussian distribution around mean particle size. For more bi- or polymodal particle size distributions, like we expected here, more complex analysis methods are required [91]. The two NP distributions were evident in the TEM images of DE MNP solutions (Figures 3.1 and 3.2).

The morphology of blank DE MNPs was then examined and compared with FITC-Dex encapsulated in DE MNPs. The ratio of the gyration radius (R_g) to the hydrodynamic radius (R_h), R_g/R_h, is characteristic to the topology of the polymer. When the radius of gyration R_g from static light scattering and the hydrodynamic radius R_h from dynamic light scattering are found to be identical for each sample investigated (a ratio of 1.0), it is characteristic for spherical shells or vesicles [92]. Because PLA-Dex-PBA is a surfactant, it can generate micelles in solution. The immediate addition of the primary emulsion to the PLA-Dex-PBA solution and immediate sonication is critical to the formation of vesicles because it interrupts micelle formation before the micelles become too stable. Waiting upwards of 10 minutes after creating the 0.1% w/v PLA-Dex-PBA solution before adding the primary emulsion and sonicating resulted in significantly larger DE MNPs ($P < 0.05$), with a higher PDI than was observed for DE MNPs after immediate addition, and an R_g/R_h ratio close to 1.7, which was characteristic of gaussian chains (Supp. Table 7.1 and Figure 7.1).

The zeta potential is a key indicator of the stability of colloidal dispersions. The magnitude of the zeta potential indicates the degree of electrostatic repulsion between similarly charged particles that are adjacent in a colloidal dispersion. Nanoparticles with a zeta potential between -10 and +10 mV are considered neutral, while nanoparticles with zeta potentials of greater than +30 mV or less than -30 mV are considered strongly cationic and strongly anionic, respectively [93]. DE MNPs were characterized to be strongly anionic. Theoretically, highly positive or highly negative values of zeta potential indicate higher stability, according to the DLVO theory [93], but from a biological standpoint, particles having high positive or negative zeta potential value are prone to fast clearance from the body [93]. The highly negative charge of DE MNPs can be attributed to the PBA on the surface. The pKa of the PBA molecules are near 8.6 [162], thus at pH ~7.2 (the pH of DE MNPs), at which the measurements were taken, some percentage of the PBA molecules would be in their deprotonated state, contributing to the overall negative surface charges of the nanoparticles. The range of zeta potentials on nanoparticles with PBA molecules on the surface in literature is approximately -30mV [94]. This is an indication that there is something else contributing to the surface charge. In order to explore this further, DE MNPs were prepared using PLA-Dex instead of PLA-Dex-PBA. Theoretically, the DE MNPs should form just as if PLA-Dex-PBA is being used, with a comparable diameter, conformation, and polydispersity which is observed. The zeta potential of the PLA-b-Dex NPs has been previously explored by the Frank Gu Research Group and found to be -2.63 ± 1.55 mV. The zeta potential of DE MNPs using PLA-Dex was significantly lower at -43.8 mV. Previous studies have shown that increase in polymer concentration or changing in the mixing mechanism does not change the zeta potential; however, changing the type and concentration of surfactants strongly affects the zeta potential [95]. This suggests that SPAN80 may be migrating to the outer surface of DE MNPs, thus contributing to the anionic charge observed.

TEM confirmed spherical shell/vesicle structures and integrity of DE MNPs to retain their shape upon drug loading. The TEM images are shown in Figure 3.1. The sizes of the DE MNPs appeared smaller in the TEM images compared to the reading estimated by the DLS. Differences in particle size from light scattering techniques versus those seen by TEM can be attributed to 2 processes. It is possible that the NPs in solution have a tendency to aggregate, or that the drying process in preparing the TEM grids shrinks the NPs as a result of evaporation [96]. Since the polydispersity of DE MNPs is quite low (below 0.1), and the DE MNPs are strongly anionic, significantly decreasing their tendency to aggregate, it is more likely that the difference in size seen between DLS and TEM is a result of the evaporation of water in the drying process.

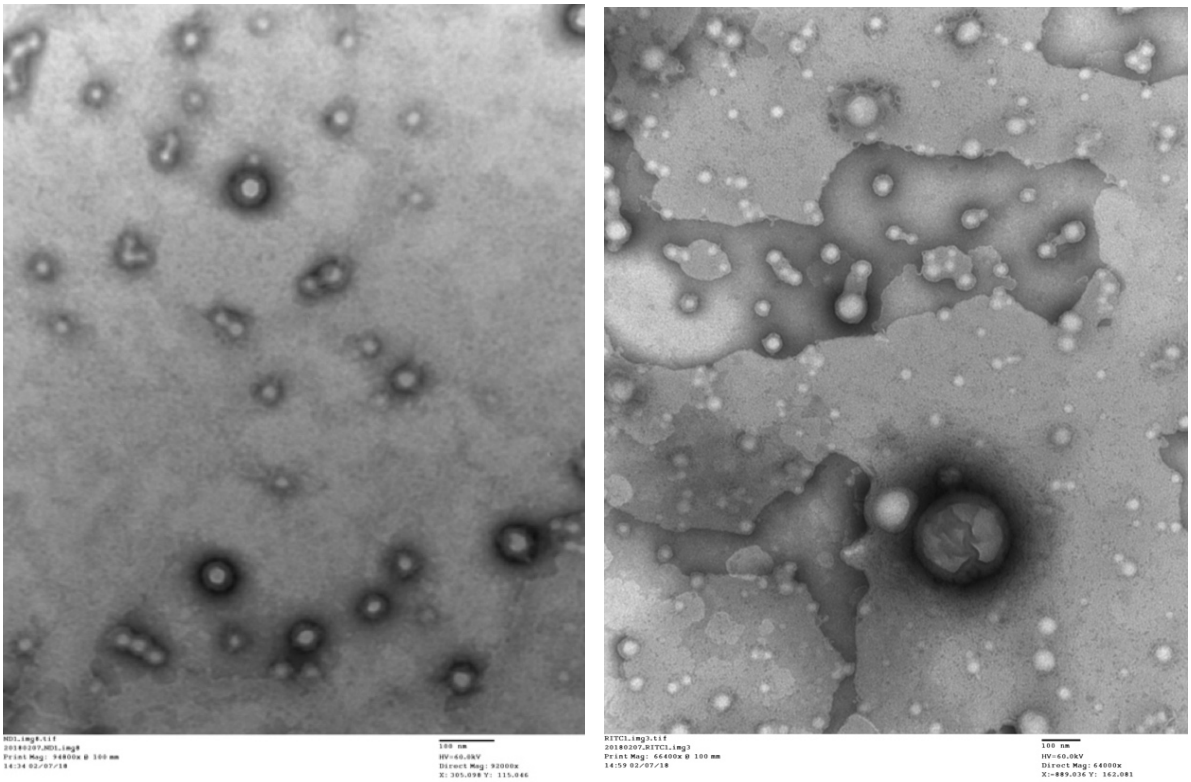

Figure 3.1 TEM images of blank DE MNPs (left: 100 nm scale bar) and FITC-Dex loaded DE MNPs (right: 100 nm scale bar) negatively stained with phosphotungstic acid.

We expected the aqueous phases to appear darker than the oil phase. It is apparent that this is not observed in Figure 3.1. In order to assess whether the explanation for this was a result of lack of double emulsion formation or merely a result of the stain not being able to penetrate into the aqueous core, phosphotungstic acid was loaded into the core of DE MNPs during the synthesis process and reimaged showing some but not all particles exhibiting a dark interior and dark exterior (Supp. Figure 7.2).

PLA-Dex-PBA block co-polymer will naturally self-assemble to form micelles in solution. In preparation of DE MNPs, this process was interrupted by the immediate addition of the primary emulsion to the solution containing 0.1% w/v PLA-Dex-PBA, and the immediate sonication to form the secondary emulsion. Because of this process, we expected to see a distribution of both micelles and double emulsions. We hypothesized that the smaller spheres in Figure 3.1 are micelles.

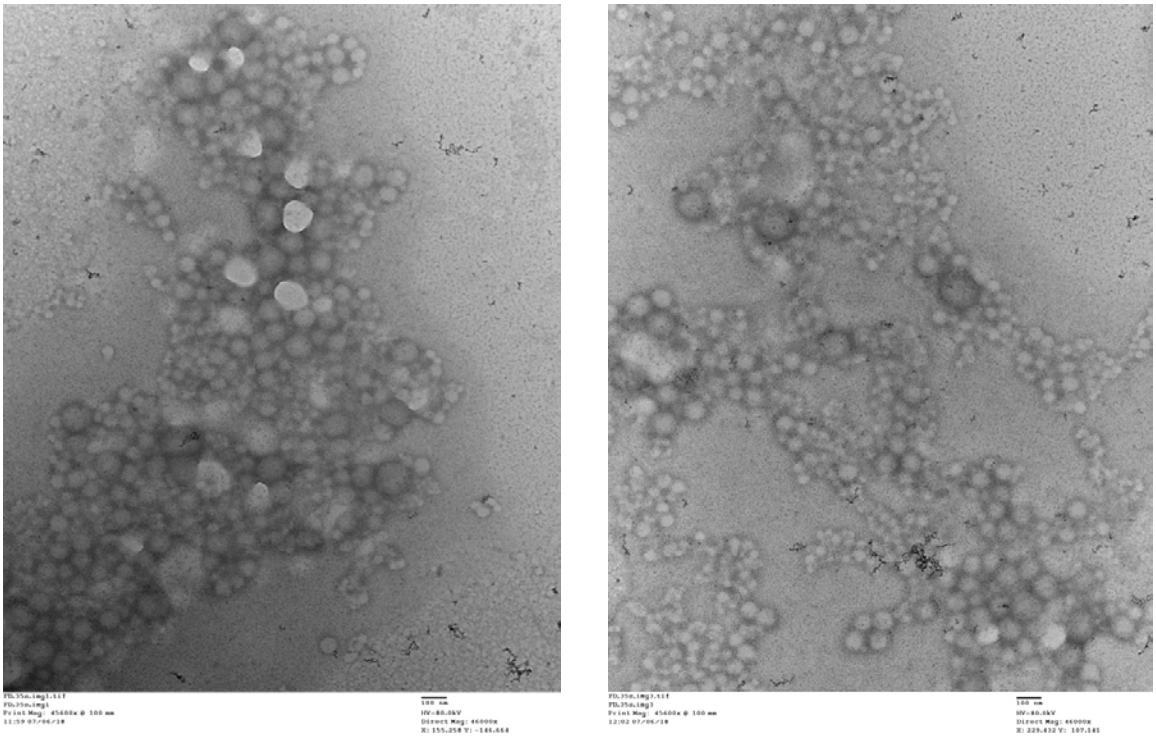

Figure 3.2 TEM images of blank DE MNPs (left: 100 nm scale bar) and FITC-Dex loaded DE MNPs (right: 100 nm scale bar) double stained with uranyl acetate and lead citrate.

Using a double staining method using uranyl acetate and lead citrate [97], the morphology of blank DE MNPs was examined and compared with FITC-Dex encapsulated in DE MNPs. In theory this method should help distinguish between the micelles and the double emulsions. Small brighter (~50nm) particles are proposed to be micelles, meanwhile the larger darker particles with a distinctly darker ring around the edges are proposed to be vesicles. In making the stain, CO_2 free water was required because lead stains are easily precipitated upon contact with CO_2 [98]. The black precipitates seen in Figure 3.2 are a result of CO_2 interacting with lead citrate.

3.4.2 Drug Loading based on WT%

FITC-Dex (10K) was encapsulated in the MNPs at three weight percentages: 10, 30, and 100%. The drug concentrations were explored to allow a better characterization of the DE MNPs' drug loading abilities. Maximum encapsulation efficiency (EE%) of FITC-Dex was achieved at an initial feed of 30 wt% with an encapsulation efficiency of approximately 87%. EE% did not change significantly when the initial wt% of FITC-Dex was tripled to 90 wt%, however, the drug loading (DL%) continued to increase,

indicating that more drug may be able to be incorporated into the formulation and higher drug percentages may be possible. This was also indicative that the PLGA-SPAN80 matrix that makes up the organic phase (the first emulsion) was viscous enough to decrease the diffusion rate of the drug from the inner aqueous phase to the external aqueous phase. This can be explained by the high molecular weight of PLGA (40-75 KDa) and the concentration of SPAN80 (5% w/v) that stabilize the first emulsion. Samples were measured by DLS for their size, and UV-Vis for their encapsulation efficiency and drug loading. It was observed that drug loading does not significantly influence mean particle size, however this has been seen before [85], [99], [100]. Typically, the size of double emulsions are influenced by the polymer (PLGA) concentration, which was only 12.5% larger for the FITC-Dex loaded samples than the blank DE MNPs. Results are shown in Table 3.2 and Figure 3.3.

Formulation	**Mean Diameter[a)] (nm)**	**Mean PDI[b)]**	**EE[c)] (%)**	**DL[d)] (%)**
Blank DE MNPs	162 ± 5	0.0935 ± 0.0201	N/A	N/A
FITC-Dex (10wt%)	157 ± 1	0.0770 ± 0.0124	57.5 ± 14.3	5.75 ± 1.44
FITC-Dex (30wt%)	156 ± 1	0.111 ± 0.0461	86.0 ± 1.3	25.8 ± 0.4
FITC-Dex (90wt%)	170 ± 8	0.0690 ± 0.0278	87.3 ± 1.9	78.6 ± 1.7

Table 3.2 Characterization of blank and FITC-Dex loaded DE MNPs at varying wt% by (a) size, (b) polydispersity index (c) encapsulation efficiency, and (d) drug loading; n = 2 ± s.e.

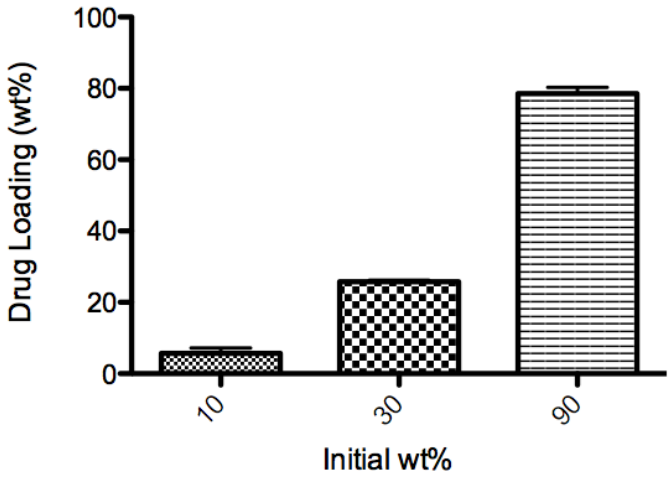

Figure 3.3 FITC-Dex loading in DE MNPs based on initial FITC-Dex wt%; n = 2 ± s.e.

3.4.3 Drug Loading based on MWt

Keeping other conditions constant, the effect of FITC-Dex molecular weight on the properties of DE MNPs was evaluated (Table 3.3 and Figure 3.4). Three different molecular weights, 3KDa, 10KDa, and 40KDa, were investigated for their drug loading abilities (initial 100 wt%). It remained true that the maximum encapsulation efficiency that can be achieved by DE MNPs is in the 80th percentile. No significant differences in particle size were observed for the 3KDa and 10KDa FITC-Dex samples ($P > 0.05$), however there was a significant increase in particle size for the 40KDa FITC-Dex sample. The sizes of double emulsions are influenced by the polymer concentration, which were not significantly different for the 3KDa FITC-Dex sample (3.75% increase), or for the 10KDa FITC-Dex sample (12.5% increase). However, the 40KDa FITC-Dex sample (50% increase) changed the polymer concentration significantly and this was observed in the change in particle size. DL% were comparable for FITC-Dex(3K) and FITC-Dex(10K) ($P > 0.05$), however, the value decreased for FITC-Dex(40K) loaded DE MNPs ($P < 0.05$). This was likely due to the long dextran chain length of FITC-Dex(40K) allowing for the formation of diffusion channels through the organic phase, leading to increased drug loss during the DCM evaporation stage [85].

Formulation	Mean Diameter[a)] (nm)	Mean PDI[b)]	EE[c)] (%)	DL[d)] (%)
Blank DE MNPs	154 ± 1	0.116 ± 0.0345	N/A	N/A
FITC-Dex (3K)	147 ± 7	0.106 ± 0.0742	83.1 ± 3.27	83.1 ± 3.27
FITC-Dex (10K)	149 ± 4	0.0710 ± 0.0216	84.1 ± 2.38	84.1 ± 2.38
FITC-Dex (40K)	162 ± 1	0.917 ± 0.0472	60.7 ± 5.36	60.7 ± 5.36

Table 3.3 Characterization of blank and FITC-Dex loaded DE MNPs at varying molecular weights by (a) size, (b) polydispersity index, (c) encapsulation efficiency, and (d) drug loading; n = 3 ± s.e.

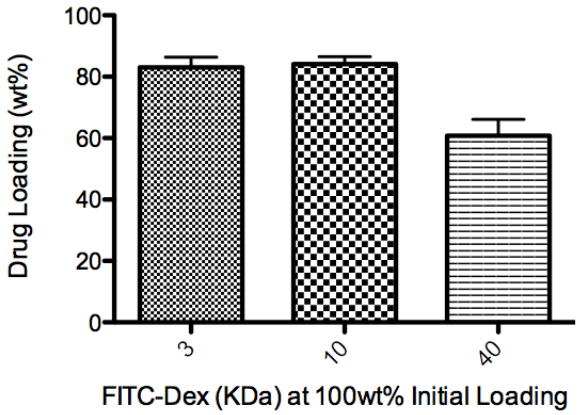

Figure 3.4 FITC-Dex loading in DE MNPs based on FITC-Dex MWt; n = 3 ± s.e

3.4.4 *In vitro* release

DE MNPs in STF at 37°C were analyzed by quantifying the FITC-Dex in the STF at predetermined time intervals using UV-Vis. DE MNPs showed total release at 168 hours, which is significantly longer than free-drug which showed total release at 24 hours (Figure 3.5). As seen in Figure 3.5, drug release from DE MNPs was slow and prolonged in comparison with FITC-Dex release from solution. The initial release after 0.5 hr from DE MNPs was 13.3% compared with the solution which released 31.2%. The release from solution increased and then plateaued at 12 hr with a cumulative release of 102.6%. On the contrary, the DE MNPs showed increase in release until 168 hr (approximately 7 days).

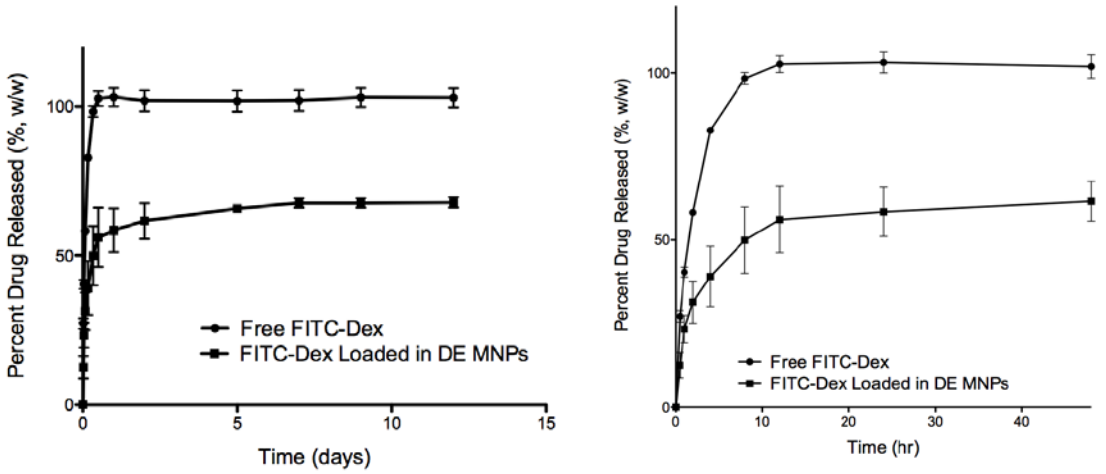

Figure 3.5 *In vitro* release of FITC-Dex from DE MNPs in STF (pH 7.4, 37 °C) over 12 days (left), over 48 hr (right); n = 3 ± s.e

There was an initial burst release of FITC-Dex, however this was 2.3x less than the initial release observed of the free-drug, suggesting that the DE MNPs retarded the release of FITC-Dex. A burst release occurs when more than 30% of the therapeutic agent contained by the drug delivery system is released from the drug delivery system within about 48 hours. Burst release can be a particular problem with water soluble drugs which have a propensity to quickly enter solution in an aqueous physiological environment [101]. We postulated that the mechanism of drug release occurs by a process of diffusion. The initial burst release can be explained by the presence of drug interacting with the surface of double emulsion nanoparticles [85], rather than/in addition to drug distributed in the internal matrix of the polymer.

The rate of release of FITC-Dex in solution was consistent, however, the rate of release of FITC-Dex from DE MNPs was faster in the first 12 hours (56.1%), and much slower in the remaining 156 hours releasing the remaining 10% of drug (for a total of 67.6%). This suggests that DE MNPs have drug both on their surface and in their core. It is possible that there was free-drug in the DE MNP solution, however, we would expect the free drugs to have a similar burst release to the FITC-Dex solution, which it did not. The

initial slower rate further supports the probability of FITC-Dex associated with the surface of DE MNPs, which are released first. The small initial burst release is undesirable; release studies using DE MNPs containing only FITC-Dex encapsulated in the core should be conducted for comparison.

The zeta potential, typically used to determine the surface charge of the particles, can be used to determine whether a charged active material is encapsulated within the center of the nanoparticle or on the surface [102].

Formulation	Diameter[a)] (nm)	PDI[b)]	R_g/R_h[c)]	ξ Potential[d)] (mV)	DL[e)] (%)
Blank DE MNPs	163	0.0870	1.22	-59.2	N/A
FITC-Dex loaded DE MNPs	160	0.112	1.21	-29.5	73.7
Blank DE MNPs post-12 hr dialysis	163	0.0490	1.21	-60.2	N/A
FITC-Dex loaded DE MNPs post-12 hr dialysis	154	0.0920	1.09	-62.9	15.7

Table 3.4 Evaluation of presence of FITC-Dex in the core vs. on the surface of DE MNPs by (a) size, (b) polydispersity index, (c) conformation, (d) surface charge, and (e) drug loading; n = 1

FITC-Dex loaded DE MNPs had a more positive zeta potential ($P < 0.05$) than blank DE MNPs, further supporting the hypothesis that some FITC-Dex was loaded on the surface of DE MNPs. Some of the FITC-Dex loaded DE MNP sample was used for characterization of size, morphology, and drug loading (Table 4.4), meanwhile the rest of the sample was subjected to dialysis for 12 hours (chosen based on release study) in an attempt to dissociate the FITC-Dex from the surface of DE MNPs. The blank DE MNPs and the FITC-Dex loaded DE MNPs post-12 hr dialysis had comparable zeta potentials ($P > 0.05$), indicating that most, if not all, FITC-Dex on the surface of DE MNPs was removed. These particles were also characterized for size, morphology, and drug loading for comparison. ND DE MNPs had comparable effective diameters, vesicle morphologies and zeta potentials before and after dialysis ($P > 0.05$). FITC-Dex DE MNPs had comparable effective diameters and vesicle morphologies before and after dialysis ($P > 0.05$), however the drug loading and the zeta potential were significantly different ($P < 0.05$). By measurement of the zeta potential, it can be determined if the drug is shielded by the nanoparticle or not because if the drug is shielded, then the zeta potential will be close to the nanoparticle zeta potential [103]. The FITC-Dex loaded DE MNP sample had comparable zeta potential to blank DE MNPs post-dialysis ($P > 0.05$) suggesting that the remaining FITC-Dex in the sample (15.7%) was shielded by the nanoparticle (located in the core). The

purpose of this thesis was not to study the effects of the process parameters on DE MNPs, however, this is something that should be considered moving forward in order to improve the DE MNP platform.

Chapter 4
Mucoadhesive abilities of DE MNPs

4.1 Summary

The mucoadhesive functionality on DE MNPs is PBA. The mucoadhesive binding occurs between the PBA grafts on the MNPs and N-Acetylneuraminic acid (sialic acid). Sialic acid (SA) is the terminal monosaccharide on the mucus membrane [104]. The binding is shown in Figure 4.1.

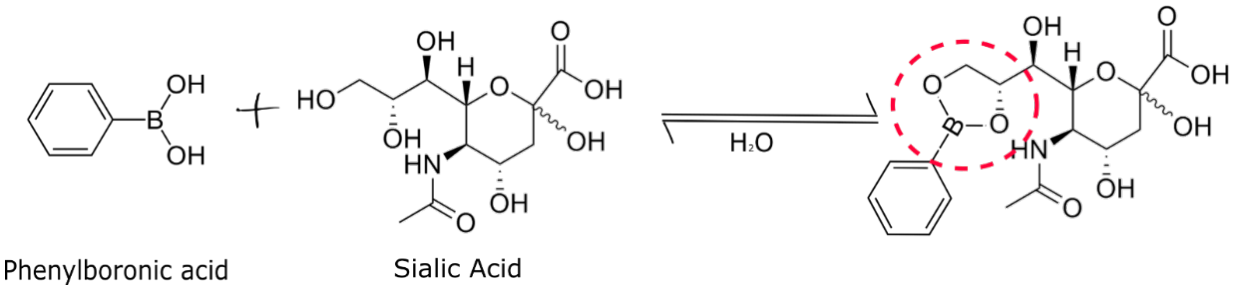

Figure 4.1. PBA binding to SA

PBA's hydroxyl groups bind to SA through covalent diol-diol binding, allowing the MNPs to stay on the mucus membrane and deliver drugs effectively over a long period of time [105]. Fluorescence binding studies between SA and DE MNPs showed mucoadhesion *in vitro*, but when evaluated for ocular retention *in vivo*, DE MNPs failed to evade clearance; which may be attributed to their large size and/or strongly anionic surface charge.

4.2 Introduction

One of the biggest challenges of ocular drug delivery is the nature of the ocular anatomy. Topical administration is the most prevalent and popular method of drug administration, however, it is very difficult to achieve therapeutic drug concentrations because of precorneal factors such as blinking, nasolacrimal drainage, and transient residence time in the cul-de-sac [1]. To overcome these barriers, mucoadhesive nanoparticles have gained a lot of popularity, increasing contact time of the nanoparticles on the ocular surface, thereby increasing the bioavailability of the encapsulated drug.

Chitosan, another biodegradable and biocompatible polymer has been investigated as a mucoadhesive functionality to decorate PLGA for more targeted binding. Chitosan functionalized PLGA, however, have been extensively used for cancer targeting or to improve oral bioavailability [106]. Phenylboronic acid (PBA) molecules have also been investigated for their mucoadhesive properties. PBA

forms a complex with cis-diol groups of sugar residues, such that they are successful at interacting with sialic acids which are abundant on the mucin structures in the eye at physiological pH [107]. In addition, several studies have demonstrated biocompatibilities of PBA molecules using both *in vitro* and *in vivo* assays [108],[109],[110].

In a previous study, phenylboronic acid has been surface functionalized on PLA-b-Dex polymers [8]. The objective of this study was to develop a mucoadhesive nanoparticle delivery system for hydrophilic drugs that can reduce the administration frequency of ophthalmic drugs without compromising the therapeutic efficacy. Here, we investigated *in vitro* mucoadhesion as a proof of concept that PBA is on the surface of DE MNPs, and *in vivo* mucoadhesion for ocular retention after administration on rabbit eyes.

4.3 Experimental Section

4.3.1 Materials

Fluorescein-isothiocyanate dextran (MW 10kDa), Poly(D,L – lactide-co-glycolide) (MW 45 kDa – 75 kDa), SPAN80®, Dimethyl sulfoxide (DMSO), Dichloromethane (DCM), Dextran (MW: 10 kDa), 3-Aminophenylboronic acid monohydrate (PBA), sodium periodate ($NaIO_4$), glycerol, sodium cyanoborohydride ($NaCNBH_3$), N-acetylneuraminic acid (SA) were purchased from Sigma Aldrich (Canada). Acid-terminated PLA (MW: 20 kDa) was purchased from Lakeshore Biomaterials (USA) and washed with methanol to remove monomer impurities.

4.3.2 Synthesis

Synthesis of a water-in-oil-in-water (W/O/W) emulsion first involved the formation of the primary emulsion (W/O). The primary emulsion was made by dissolving FITC-Dex (10mg/mL) in 0.4mL of MilliQ and that to 2mL of 10mg/mL PLGA dissolved in DCM containing 5% w/v SPAN80. DCM and MilliQ are immiscible liquids that require ultrasonification to homogenize. Using the Fischer Scientific Branson Probe Sonicator, the mixture was sonicated for 30 seconds (pulse 0.2, amplitude 30) to obtain a primary water-in-oil emulsion [83].

The primary emulsion was then added to a larger aqueous phase containing a surfactant in order to produce the secondary emulsion (W/O/W). The surfactant used in this phase was the amphiphilic block copolymer PLA-Dex-PBA which was prepared using a previously reported method [106]. In brief, PLA-Dex-PBA was synthesized by dissolving PLA-Dex in DMSO (30 mg/ml), and added slowly into water under mild stirring. Oxidation of the dextran surface was carried out by adding 60mg of sodium periodate ($NaIO_4$) and stirring for an hour. Subsequently, glycerol was added to quench the unreacted $NaIO_4$. Surface functionalization with PBA was carried out using reductive amination in the presence of $NaBH_3CN$ for

24 hours. The mixture was then dialyzed in H_2O for 24 hr to remove any unreacted solutes, changing the wash medium 4 times. All reactions were carried out in dark [106].

To generate the second emulsion, PLA-Dex-PBA was dissolved in DMSO (12.5mg/mL) and added dropwise to 12.5 mL of MilliQ under vortex to generate a 0.1% w/v PLA-Dex-PBA solution. The primary emulsion was then immediately added to the 0.1% w/v PLA-Dex-PBA solution and homogenized using the Fischer Scientific Branson Probe Sonicator for 30 seconds (pulse 0.2, amplitude 30) to obtain a water-in-oil-in-water emulsion. The mixture was left to evaporate the organic solvent overnight while under stirring (490rpm) then dialyzed in 1L of DI H_2O the next morning using 12-14K molecular weight cut-off (MWCO) dialysis tubing for 1.5 hours to remove the DMSO. To make blank DE MNPs, the same process was followed, however 0.4mL of MilliQ was used to generate the first emulsion.

4.3.3 Characterization of PLA-Dex-PBA DE MNPs

The mean particle diameter and polydispersity index was determined using Dynamic Light Scattering (DLS) by measuring the Multimode-Size Distribution (MSD) volume-averaged mean diameters using a 90Plus Particle size Analyzer (Brookhaven, λ = 636 nm at 90°). The analysis was performed at room temperature, at a scattering angle of 90°C. DE MNPs were filtered through a syringe filter (pore size = 200nm) to remove the drug and NP aggregates, then diluted 20x prior to analysis. The zeta potential of the Control (no drug) DE MNP and the drug containing (encapsulated) DE MNP were measured using Zetasizer Nano ZS (Malvern Instruments Worcestershire, U.K.) using 200nm filtered sample. The sizes and morphology were further analyzed by Static Light Scattering (SLS). SLS measurements were processed in batch mode using a multi angle laser light scattering apparatus (Brookhaven BI-200SM Laser Light Scattering System) equipped with a 25mW Ga/As laser beam operating at λ = 636 nm. Light scattering intensities recorded at 5 angles between 45° and 155° were derived with the ASTRA software according to the Zimm procedure. The sensitivity of the SLS is greater than the DLS, thus the DE MNPs were further diluted 50x prior to analysis. Measurements of hydrodynamic radius (R_h) and radius of gyration (R_g) were obtained and used to assess DE MNP conformation.

4.3.4 FITC-Dex encapsulation

The encapsulation of FITC-Dex in the DE MNPs was accomplished by dissolving the hydrophilic (model) drug in MilliQ for the aqueous phase in the primary emulsion. The DE MNPs, post dialysis, were filtered through a syringe filter (pore size 200nm) to remove the drug and NP aggregates. The NPs were subsequently filtered through Amicon filtration tubes (MWCO = 30 kDa, Millipore for 3kDa and 10kDa FITC-Dex loaded DE MNPs, MWCO = 100 kDa, Millipore for 40kDa FITC-Dex loaded DE MNPs) to further remove any

remaining free drugs in the suspension. The filtered DE MNPs containing encapsulated FITC-Dex were re-suspended and diluted in DMSO. The drug loading (wt%) in the polymer matrix was calculated by measuring the concentration of FITC-Dex in the solution by obtaining the absorbance at 518nm using Epoch Multi-Volume Spectrophotometer System (Biotek). The measurements were obtained in triplicate (n=3, mean ± S.D). The absorbance measured by the same procedure using DE MNPs without encapsulated drug was used as the baseline. The absorbance was correlated using a standard calibration curve of FITC-Dex in DMSO. The encapsulation efficiency (%) and drug loading (wt%) were calculated using the two equations below.

$$\mathrm{EE\%} = \frac{[\mathrm{Drug}]_{\mathrm{actual}}}{[\mathrm{Drug}]_{\mathrm{theoretical}}} \times 100\%$$

Equation 1. Encapsulation efficiency

$$\mathrm{DL\%} = \mathrm{EE} \times \mathrm{DL\%}_{\mathrm{theoretical}}$$

Equation 2. Drug Loading

4.3.5 *In vitro* mucoadhesion via Fluorescence

Fluorescence studies were conducted in order to evaluate the mucoadhesive properties of DE MNPs. This was done by determining the covalent interaction between the PBA grafts on the surface of DE MNPs and sialic acid (SA) molecules. The interaction of these two molecules quenches the intrinsic fluorescence of PBA, therefore, the interaction between PBA and SA can be quantified by analyzing the relative fluorescence intensities of DE MNPs in the presence of varying concentrations of SA. The relative fluorescence data can then be analyzed to determine the Stern-Volmer binding constant [110], K_{SV}, using the Stern-Volmer equation as seen in Equation 3 below,

$$\frac{I_0}{I} = 1 + K_{sv} \times [Q]$$

Equation 3. Stern-Volmer equation

where I_0 is the fluorescence intensity of the DE MNPs sample without SA ([SA] = 0 mM), I is the fluorescence intensity of DE MNPs with SA, and [Q] is the concentration of the quenching agent, SA. The K_{SV} value is determined by calculating the slope of the linear fit.

DE MNP suspensions were mixed with SA solutions to achieve a constant final concentration of DE MNPs (20 μg/ml) with varying SA concentrations (0, 10, 30, 60, 100, 150, and 200 mM). The samples were excited at 298 nm, and the emission scan from 330 to 450 nm was obtained for each sample. The

relative fluorescence data was then analyzed to determine K_{SV} using the Stern-Volmer equation. The mixtures were vortexed for 30 seconds before measurement, with the same parameters used.

4.3.6 *In vivo* mucoadhesion via Ocular Retention

All animal studies performed were in compliance with the guidelines of the Canadian Council on Animal Care (CCAC) and the University of Waterloo (UW) as well as regulations under the Animals for Research Act of Ontario Canada. Three male New Zealand White Albino rabbits (2.5 – 3.5 kg, Charles River Laboratories, Canada) were used for this study. FITC-Dex was encapsulated in the NPs and administered to rabbit eyes to track its ocular retention. At predetermined time intervals, images were taken using a confocal scanning laser ophthalmoscope (cSLO) of each of the rabbits' eyes. 50μL of FITC-Dex encapsulated DE MNPs was administered in one eye, and 50μL of FITC-Dex (at the concentration which was encapsulated in the DE MNPs) was administered in the other for comparative analysis. All animals were acclimated in the animal facility for at least one week prior to the experiments. All formulations used in this study were dialyzed, filtered, and sterilized prior to administration to the animals.

4.4 Results & Discussion

4.4.1 Characterization and Drug Loading

DE MNPs were synthesized for the purpose of mucoadhesion studies. Blank DE MNPs were used for *in vitro* fluorescence binding studies, meanwhile FITC-Dex loaded DE MNPs were used to evaluate *in vivo* mucoadhesion and ocular retention (Table 4.1). Sizes of blank DE MNPs and FITC-Dex loaded DE MNPs were comparable ($P > 0.05$), with similar R_g/R_h ratios and DL% observed during development studies discussed in Chapter 3.

Formulation	Mean Diameter[a)] (nm)	Mean PDI[b)]	R_g/R_h[c)]	DL[d)] (%)
Blank DE MNPs	150 ± 2	0.0957 ± 0.0875	1.21 ± 0.03	N/A
FITC-Dex Loaded DE MNPs	152 ± 3	0.0980 ± 0.0649	1.02 ± 0.09	84.8 ± 1.1

Table 4.1 Characterization of blank and FITC-Dex loaded DE MNPs by (a) size, (b) polydispersity index, (c) conformation, and (d) drug loading; n = 3 ± s.e.

4.4.2 *In vitro* mucoadhesion

To quantitatively evaluate the mucoadhesive properties of DE MNPs, the covalent interaction between the PBA grafts on the surface of the MNPs and sialic acid (SA) molecules was studied using fluorescence [110]. The covalent complexation between PBA and SA quenches the intrinsic fluorescence of the PBA

molecules. Thus, the interaction between PBA and SA can be quantified by analysing the relative fluorescence intensities of MNPs in the presence of varying concentrations of SA. Blank DE MNPs were used for this study such that no other fluorescent moieties could skew the data.

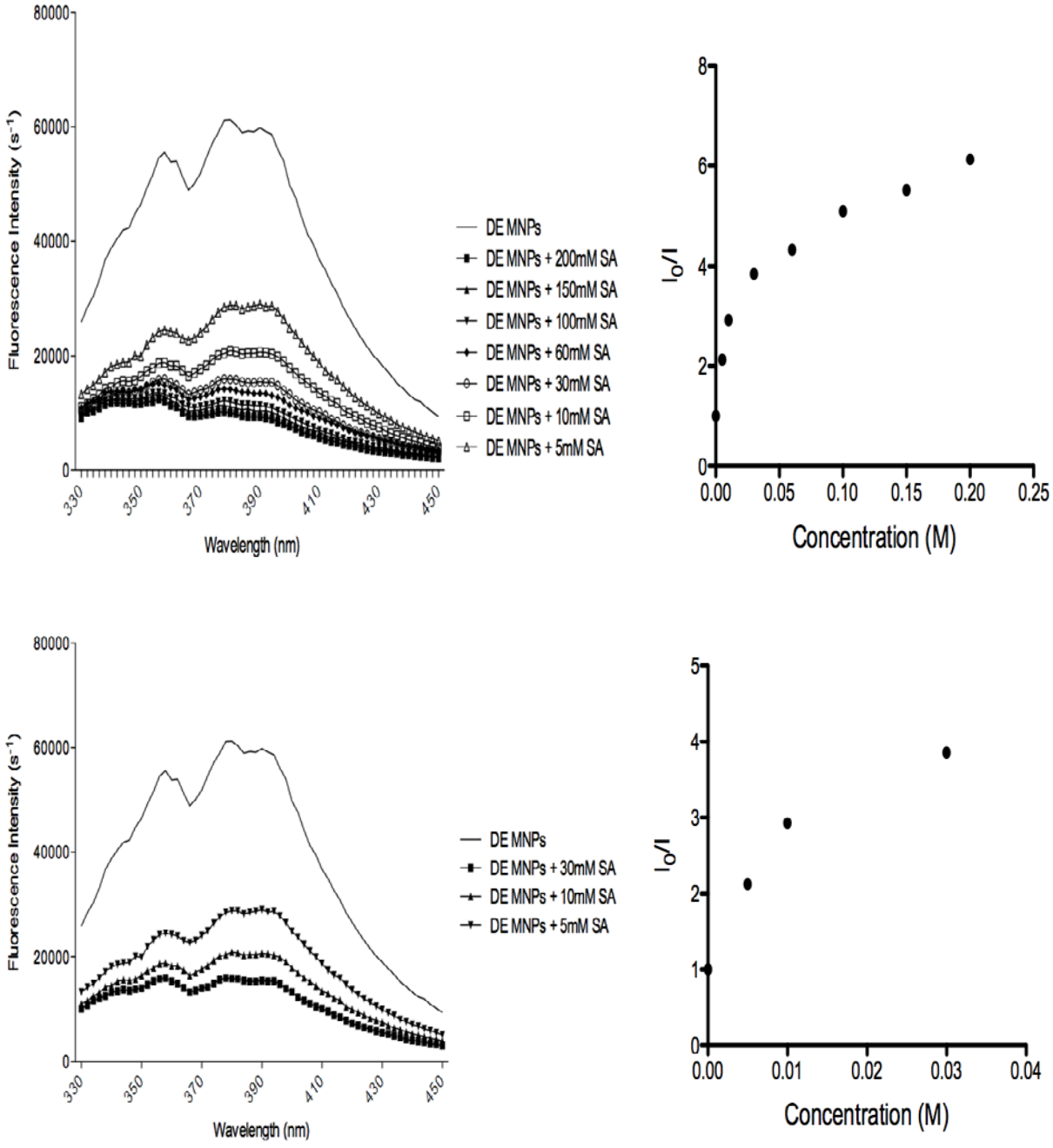

Figure 4.2 Fluorescence emission spectra and analysis DE MNP-SA binding. SA concentrations used past the saturation point skew results. Top left and right show the emission spectra and analysis with a wide range of SA concentrations, going past the saturation point, where large increases in SA do not significantly change the fluorescence. Bottom left and right show the emission spectra and analysis of MNP-SA binding below the saturation point.

The emission spectra (Figure 4.2, left) show decreasing fluorescence intensity with increasing SA concentrations as expected. I_0/I vs [SA] was plotted for each SA concentration, and the data was fit to the Stern-Volmer equation through linear regression (Figure 4.2, right). This yielded a K_{SV} value which is also known as a binding constant. The PBA-SA quenching occurs through photoinduced electron transfer, where the electron excited in the PBA is transferred to SA instead of being emitted. The type of fluorescence quenching that was being evaluated here is static quenching which yields a K_{SV} equal to K_A, the association constant. Dynamic quenching (when the quencher interferes with the excited state after formation) yields a K_{SV} which is its own binding constant, similar but not equivalent to K_A [110]. Static quenching allows us to make comparisons between the K_{SV} value determined from this method and the literature sources of K_A for PBA-SA binding [111], [112].

The analysis for K_{SV} ends at the SA concentration after which the DE MNP solution becomes saturated with quencher (i.e. adding more quencher does not significantly change the fluorescence intensity). High concentrations cause a plateau to be formed in the analysis on the right; linear regression cannot be performed on this data. If concentrations of SA above the saturation point are used, linear regression is not accurate and the resulting K_{SV} value is very different. However, looking at data below the saturation point, we see that the trend appears to be more linear and it is at these concentrations that we can obtain an accurate binding constant. Careful consideration must be taken to avoid using concentrations above the saturation point (which is usually noted qualitatively from the emission spectra and the graphical analysis), or else the reported data will be incorrect. Though disregarding the data points above the saturation point does give a more linear relationship, repeats of this study at lower concentrations (below saturation) should be conducted. We hypothesize that then, the K_{SV} calculated from linear regression will be more precise and reflective of the binding between PBA and SA.

Literature values place the KA for PBA-SA between 11.4 M^{-1} – 37.6 M^{-1} depending on the method used to determine it [113], [108], [114]. We expect the calculated K_{SV} to be higher than this documented range as a result of the high number of PBA molecules decorating the surface of the DE MNPs. Previously reported K_A values measuring PBA binding with sialic acid typically have one PBA moiety per compound [110], [108], whereas DE MNPs have a high number, 17.0 mol%, on the dextran monomer). This makes DE MNPs much more likely to bind to SA, as they have more binding sites available per NP.

4.4.3 *In vivo* mucoadhesion

The results in section 4.4.2 confirmed that it was possible to quantify the binding between DE MNPs and SA, alluding to PBA being the mucoadhesive component of DE MNPs, and to PBA likely being on the surface of DE MNPs. This prompted us to evaluate the mucoadhesive properties of DE MNPs *in vivo*. To do this, ocular retention of DE MNPs on the corneal surface of rabbit eyes was measured using cSLO.

Standardized images SLO (Figure 4.3) showed that the FITC-Dex delivered using DE MNPs demonstrated lower retention of FITC-Dex compared to the FITC-Dex control, which was especially noticeable at the 3 hr time-point (Figure 4.3).

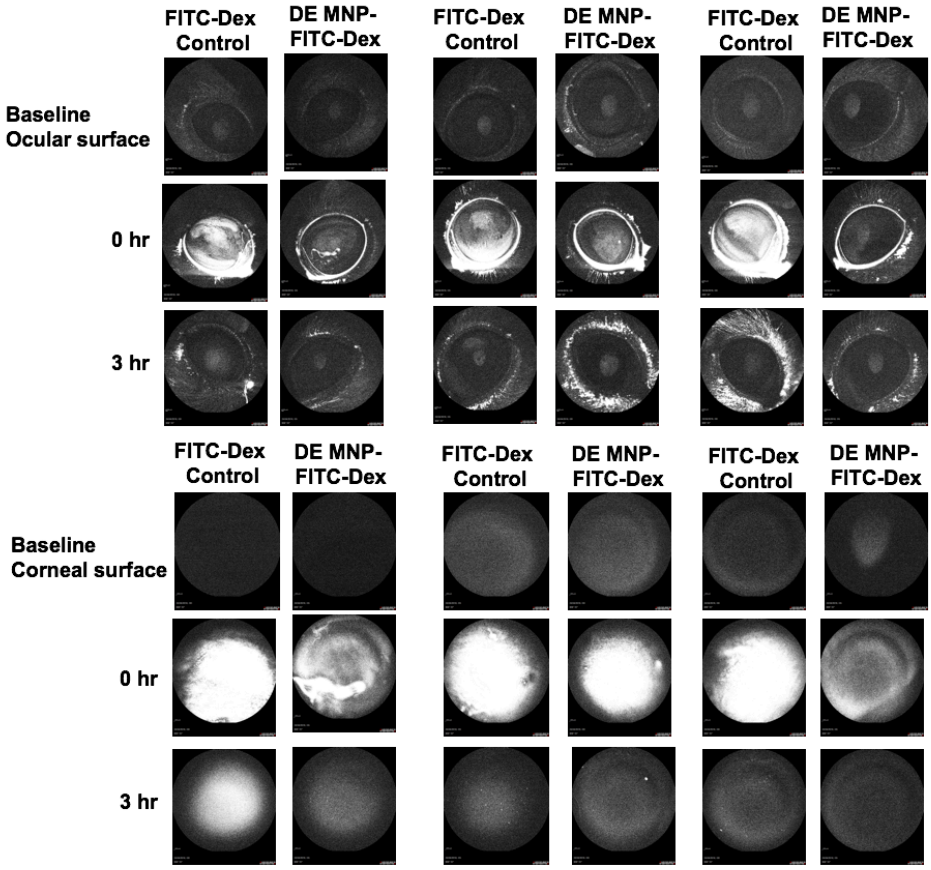

Figure 4.3 Fluorescence images of NZW rabbit eyes treated with FITC-Dex and FITC-Dex loaded DE MNPs taken using confocal Scanning Laser Ophthalmoscopy (cSLO).

Though DE MNPs show smaller particle sizes than what was typically observed for double emulsions using PLGA in literature [85], [86], [90], DE MNPs are significantly larger than PLA-Dex-PBA MNP micelles [8]. ICG delivered via PBA modified PLA-b-Dex micelles showed ocular retention beyond 24 hours on rabbit eyes, whereas free ICG was mostly cleared within the first 3 hours [105]. DE MNPs should hypothetically show similar ocular retention, but the fact that they did not may be attributed to particle size and surface charge. Larger NPs cause more irritation and discomfort than smaller NPs, stimulating reflex tearing and inducing a more rapid clearance [82]. Furthermore, the corneal surface contains negatively charged ocular mucin [115]. From the zeta potential data, it was learned that DE MNPs are strongly anionic, especially in comparison to their micelle counter-parts which showed zeta potentials close to 0 mV. This would cause the DE MNPs to be repelled by the negatively charged mucin and result in rapid clearance of the drug carrier. These factors individually can decrease the ocular retention of DE MNPs, and together can

explain the rapid clearance of DE MNPs from the ocular surface, despite the presence of PBA on the surface. Furthermore, it is possible that PBA is not doing its job as the mucoadhesive component of DE MNPs. High affinity SA-PBA complexation might not occur in a physiological environment, such as that of a rabbit's eye, where most SA moieties are α-SA moieties [116]. Binding properties of SA to PBA arise from ester bond formation involving the α-carboxylate moieties of β-SA but not α-SA because the binding site responsible for high-affinity binding is blocked by a glycoside bond [116]. Therefore, though we think PBA is mucoadhesive, we are not sure that this property is retained *in vivo*. Further work needs to be done to investigate the interaction of DE MNPs with ocular mucin.

Chapter 5
Applications of DE MNPs *in vitro*

5.1 Summary

Mucoadhesive NP drug carriers have attracted substantial interest as a potential solution to the low bioavailability of topical formulations. In this study, NPs composed of a PLGA core and PLA-Dex-PBA shell were developed as mucoadhesive NP drug carriers (DE MNPs). The DE MNPs encapsulated 1% w/v active PVP-I and showed that this concentration is sufficient at eradicating a bacterial culture of Escherichia coli. Current formulations such as Betadine® use 5%w/v PVP-I for treatment of ocular infection due to rapid clearance [117]. These data show that the amount of PVP-I currently used in ocular formulations can be reduced and just as effective in application, should the mucoadhesive capabilities of DE MNPs *in vivo* be improved.

5.2 Introduction

Polyvinylpyrrolidone-Iodine (PVP-I) has gained a lot of popularity in the last decade due to its affordability and its very broad antimicrobial spectrum, including bacteria, viruses, and fungi. It has been used preoperatively and post-operatively in ocular surgery and shown efficacy in reducing bacterial colony formation [117]; it has also been shown to be effective on the cervix and vagina in gynecological cases [118]. Povidone-iodine interacts strongly to the double bonds of saturated fatty acids in the bacterial cell wall and cell organelle membranes and also oxidizes amino acids and nucleotides, causing pore formation in the lipid membrane [119].

Povidone-iodine has found several applications in ophthalmology both in prevention of infections, and in the treatment of ongoing ocular infections. It has been employed preoperatively in an attempt to reduce the incidence of postoperative infections, such as endophthalmitis. PVP-I has also been popularly used as a topical antimicrobial agent effective in treating conjunctivitis and keratoconjunctivitis [118]. Furthermore, PVP-I has been used in the prevention of ophthalmia neonatorum, and as a means for decontamination of donor corneas [118].

One of the biggest challenges of ocular drug delivery is the nature of the ocular anatomy. Topical administration is the most prevalent and popular method of drug administration, however, it is very difficult to achieve therapeutic drug concentrations because of precorneal factors such as blinking, nasolacrimal drainage, and transient residence time in the cul-de-sac [1]. It has been reported that 5% PVP-I drops are only suitable for use after a local anaesthetic, as instillation causes stinging and an acute red eye. Concentrations of 1% to 1.25% PVP-I cause transient stinging. If used for bacterial conjunctivitis, compliance with the 2.5% drop would be low, the 1% strength would be tolerable [120].

The objective of this study was to test the feasibility of DE MNPs to encapsulate PVP-I, a very effective antimicrobial agent used to treat bacterial and viral infections in the eye, and exhibit antimicrobial activity *in vitro* when released from DE MNPs. By encapsulating PVP-I we would be able to not only protect the drug from clearance, but also protect the eye from the stinging effects of PVP-I. Ideally, encapsulating a clinically relevant amount of PVP-I would minimize the stinging effect of the iodine on patients because PVP-I would be protected in biocompatible NPs, while still having a therapeutic effect.

5.3 Experimental Section

5.3.1 Materials

Polyvinylpyrrolidone-Iodine (MW 40 kDa), Poly(D,L – lactide-co-glycolide) (MW 45 kDa – 75 kDa), SPAN80®, Dimethyl sulfoxide (DMSO), Dichloromethane (DCM), Dextran (MW: 10 kDa), 3-Aminophenylboronic acid monohydrate (PBA), sodium periodate ($NaIO_4$), glycerol, sodium cyanoborohydride (NaCNBH3), N-acetylneuraminic acid (SA) were purchased from Sigma Aldrich (Canada). Acid-terminated PLA (MW: 20 kDa) was purchased from Lakeshore Biomaterials (USA) and washed with methanol to remove monomer impurities. Escherichia coli (ATCC 10798) was purchased from Cedarlane Laboratories (CAN).

5.3.2 Synthesis

Synthesis of a water-in-oil-in-water (W/O/W) emulsion first involved the formation of the primary emulsion (W/O). The primary emulsion was made by dissolving PVP-I (10mg/mL) in 0.4mL MilliQ and adding that to 2mL of 10mg/mL PLGA dissolved in DCM containing 5% w/v SPAN80. DCM and MilliQ are immiscible liquids that require ultrasonification to homogenize. Using the Fischer Scientific Branson Probe Sonicator, the mixture was sonicated for 30 seconds (pulse 0.2, amplitude 30) to obtain a primary water-in-oil emulsion [83].

The primary emulsion was then added to a larger aqueous phase containing a surfactant in order to produce the secondary emulsion (W/O/W). The surfactant used in this phase was the amphiphilic block copolymer PLA-Dex-PBA which was prepared using a previously reported method [106]. In brief, PLA-Dex-PBA was synthesized by dissolving PLA-Dex in DMSO (30 mg/ml), and added slowly into water under mild stirring. Oxidation of the dextran surface was carried out by adding 60mg of sodium periodate ($NaIO_4$) and stirring for an hour. Subsequently, glycerol was added to quench the unreacted $NaIO_4$. Surface functionalization with PBA was carried out using reductive amination in the presence of $NaBH_3CN$ for 24 hours. The mixture was then dialyzed in H_2O for 24 hr to remove any unreacted solutes, changing the

wash medium 4 times. All reactions were carried out in dark [106].

To generate the second emulsion, PLA-Dex-PBA was dissolved in DMSO (12.5mg/mL) and added dropwise to 12.5 mL of MilliQ under vortex to generate a 0.1% w/v PLA-Dex-PBA solution. The primary emulsion was then immediately added to the 0.1% w/v PLA-Dex-PBA solution and homogenized using the Fischer Scientific Branson Probe Sonicator for 30 seconds (pulse 0.2, amplitude 30) to obtain a water-in-oil-in-water emulsion. The mixture was left to evaporate the organic solvent overnight while under stirring (490rpm) then dialyzed in 1L of DI H_2O the next morning using 12-14K molecular weight cut-off (MWCO) dialysis tubing for 1.5 hours to remove the DMSO. To make blank DE MNPs, the same process was followed, however 0.4mL of MilliQ was used in the generation of the first emulsion.

5.3.3 Characterization of PLA-Dex-PBA DE MNPs

The mean particle diameter and polydispersity index was determined using Dynamic Light Scattering (DLS) by measuring the Multimode-Size Distribution (MSD) volume-averaged mean diameters using a 90Plus Particle size Analyzer (Brookhaven, λ = 636 nm at 90°). The analysis was performed at room temperature, at a scattering angle of 90°C. DE MNPs were filtered through a syringe filter (pore size = 200nm) to remove the drug and NP aggregates, then diluted 20x prior to analysis. The zeta potential of the Control (no drug) DE MNP and the drug containing (encapsulated) DE MNP were measured using Zetasizer Nano ZS (Malvern Instruments Worcestershire, U.K.) using 200nm filtered sample. The sizes and morphology were further analyzed by Static Light Scattering (SLS). SLS measurements were processed in batch mode using a multi angle laser light scattering apparatus (Brookhaven BI-200SM Laser Light Scattering System) equipped with a 25mW Ga/As laser beam operating at λ = 636 nm. Light scattering intensities recorded at 5 angles between 45° and 155° were derived with the ASTRA software according to the Zimm procedure. The sensitivity of the SLS is greater than the DLS, thus the DE MNPs were further diluted 50x prior to analysis. Measurements of hydrodynamic radius (R_h) and radius of gyration (R_g) were obtained and used to assess DE MNP conformation. These findings were also confirmed using Transmission Electron Microscopy (TEM) equipment by drying the DE MNP suspension on 300 Mesh Formvar coated copper grids (Canemco and Marivac) and using phosphotungstic acid solution as the negative stain. TEM findings were further explored using a double staining method by drying the DE MNP suspension on 300 Mesh Formvar coated copper grids (Canemco and Marivac) and using lead citrate followed by uranyl acetate to stain the particles.

5.3.4 PVP-I encapsulation

The encapsulation of PVP-I in the DE MNPs was accomplished by dissolving the hydrophilic drug in MilliQ for the aqueous phase in the primary emulsion. The DE MNPs, post dialysis, were filtered through a syringe filter (pore size 200nm) to remove the drug and NP aggregates. The NPs were subsequently filtered through Amicon filtration tubes (MWCO = 100 kDa, Millipore) to further remove any remaining free drugs in the suspension. The filtered DE MNPs containing encapsulated PVP-I were re-suspended and diluted in DMSO. The drug loading (wt%) in the polymer matrix was calculated by measuring the concentration of PVP-I in the solution by obtaining the absorbance at 288nm using Epoch Multi-Volume Spectrophotometer System (Biotek). The measurements were obtained in triplicate (n=3, mean ± S.D). The absorbance measured by the same procedure using DE MNPs without encapsulated drug was used as the baseline. The absorbance was correlated using a standard calibration curve of PVP-I in DMSO. The encapsulation efficiency (%) and drug loading (wt%) were calculated using the two equations below.

$$\mathrm{EE\%} = \frac{[\mathrm{Drug}]_{\mathrm{actual}}}{[\mathrm{Drug}]_{\mathrm{theoretical}}} \times 100\%$$

Equation 1. Encapsulation efficiency

$$\mathrm{DL\%} = \mathrm{EE} \times \mathrm{DL\%}_{\mathrm{theoretical}}$$

Equation 2. Drug Loading

5.3.5 Bacterial assay

Briefly, a trypticase soy agar plate was inoculated with bacterial strain *E coli* (ATCC 10798) under aseptic conditions and incubated at 37°C for 24 hours. After 24 hours, the colony agar was used to prepare a bacterial suspension with the turbidity of 1.0 McFarland (equal to 1.0×10^9 colony-forming units (CFU)/ml), by washing *E coli* with 0.85% saline (for 3 consecutive washes and centrifugations). Turbidity of the bacterial suspension was measured at 600 nm. This was further diluted to make two concentrations of *E coli*, one with 1.0×10^7 cfu/mL and one with 1.0×10^5 cfu/mL. 100µL of bacterial suspension was mixed with 100µL of DE MNPs (0 hr – measured OD_{600}) and incubated at 37°C for 6 hours (measured OD_{600}). 25µL of this suspension was added to a trypticase soy agar plate and incubated at 37°C for 24 hours (measured OD_{600}). Quantitative measurements were obtained via OD_{600} absorbance reading and qualitative measurements were obtained through observation of bacterial growth or lack thereof. 100µL bacterial suspension mixed with 100µL of MilliQ was used as the negative standard while 100µL bacterial suspension mixed with 100µL of free drug (PVP-I) was used as a positive standard. All formulations used

in this study were dialyzed, filtered, and sterilized prior to inoculation with bacterial strain. All tests were performed in triplicate.

5.4 Results and Discussion

5.4.1 Characterization and Drug Loading

In order to assess the application of DE MNPs, Polyvinylpyrrolidone-Iodine (also known as povidone-iodine, PVP-I), was encapsulated and tested for *in vitro* anti-microbial activity. In PVP-I, polyvinylpyrrolidone is a polymer, similar to dextran, that is complexed by iodine such that a proton is fixed via a short hydrogen bond between 2 carbonyl groups of two pyrrolidone rings, and a triiodide anion is bound ionically to this cation [5] (figure 5.1).

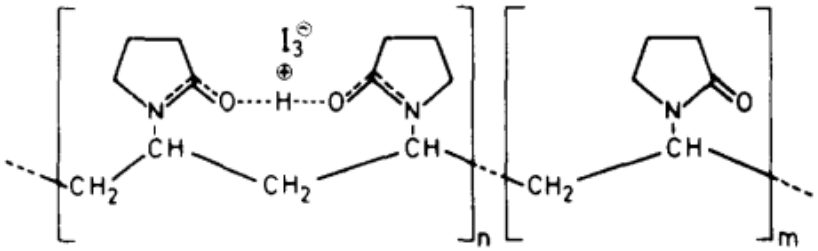

Figure 5.1 Chemical structure of polyvinylpyrrolidone-iodine (PVP-I). Reprinted from [5]**.**

Polyvinylpyrrolidone, the hydrophilic polymer that acts as a carrier in povidone-iodine, does not have any intrinsic antibacterial activity, but by virtue of its affinity to cell membranes, it delivers diatomic free iodine (I_2) directly to the bacterial cell surface [119]. Iodine's targets are located in the bacterial cytoplasm and cytoplasmic membrane, and its killing action takes place in a matter of seconds. In contact with polyvinylpyrrolidone-iodine, sulfhydry1 compounds, peptides, proteins, enzymes, vitamin C, lipids, and cytosine are iodinated and oxidated by free iodine, resulting in inactivation of molecules that are essential for biologic viability [121]. PVP-I has gained a lot of popularity in the last decade due to its affordability and its very broad antimicrobial spectrum, including bacteria, viruses, and fungi. It has been used preoperatively and post-operatively in ocular surgery and shown efficacy in reducing bacterial colony formation [117].

Formulation	Mean Diameter[a)] (nm)	Mean PDI[b)]	R_g/R_h[c)]	DL[d)] (%)
Blank DE MNPs	167 ± 1	0.104 ± 0.0570	1.01 ± 0.05	N/A
PVP-I Loaded DE MNPs	172 ± 1	0.0970 ± 0.0841	1.19 ± 0.05	7.55 ± 1.56

Table 5.1 Characterization of blank and PVP-I loaded DE MNPs by (a) size, (b) polydispersity index, (c) conformation, and (d) drug loading; n = 3 ± s.e.

The PVP-I encapsulated DE MNPs were characterized for size, morphology and drug loading (Table 5.1). The sizes of PVP-I loaded DE MNPs were significantly larger ($P < 0.05$) from blank (no drug) DE MNPs. PVP-I has a molecular weight of 40KDa. This trend was also observed for FITC-Dex at the same molecular weight (40KDa) and can be attributed to the significant increase (50%) in polymer concentration. The morphology of blank DE MNPs was examined and compared with PVP-I encapsulated in DE MNPs. The ratio of the gyration radius (R_g) to the hydrodynamic radius (R_h) were found to be identical for each sample investigated (a ratio of 1.0), supporting the spherical shell/vesicle structure of the DE MNPs with and without drug loaded. Finally, the drug loading was examined and found to be quite low at 7.55 ± 1.56 % (42μg/mL of PVP-I = 1% w/v). The documented minimum inhibitor concentration (MIC) for PVP-I with *E coli* is 34mg/L [122]. This puts the concentration of PVP-I encapsulated in DE MNPs just above the MIC, promising bactericidal activity despite the low drug loading observed. This low drug loading is likely a result of the physical characteristics of PVP-I. Because of the nature of the structure of PVP-I, only the triiodide ion had fluorescent properties that allowed us to examine and quantify the amount of drug present in the DE MNPs. The triiodide ion is electrostatically bound to PVP by hydrogen bonding and therefore easily dissociates from PVP in solution. A free-drug dialysis test suggested that 43.8% of the triiodide ion gets dissociated in just 1.5 hr (Supp. Figure .3). The triiodide ion is the most important part of PVP-I because it's the iodine that elicits the antimicrobial activity.

5.4.2 Bacterial Assay

We tested whether the amount of PVP-I (1% w/v) that was being encapsulated was significant enough to elicit bactericidal activity. Escherichia coli was used in this study at two concentrations: 1.0×10^7 cfu/mL and 1.0×10^5 cfu/mL. Bactericidal activity was monitored both qualitatively (visible growth or no growth on agar plates), and quantitatively via optical density at wavelength 600 (OD_{600}). OD_{600} values can be used to measure turbidity which in turn is used to estimate the growth phase of the population (concentration of bacteria in the solution) [123]. The higher the concentration of bacteria in a liquid culture, the higher the optical density of that culture when measured. Theoretically, the OD_{600} should decrease upon bacterial cell death [123].

Blank DE MNPs and DE MNPs loaded with PVP-I were the two experimental groups. PVP-I at the concentration loaded in the DE MNPs and Millipore H_2O were the positive and negative controls, respectively. Statistical analysis shows that there was a significant decrease in the OD_{600} of the samples containing PVP-I loaded DE MNPs and PVP-I control ($P < 0.0001$), meanwhile there was no significant change in the samples containing blank DE MNPs or Millipore H_2O ($P > 0.05$). Furthermore, the data show that there was a significant decrease in the OD_{600} of the samples containing PVP-I loaded DE MNPs

and Blank DE MNPs ($P < 0.05$). These data are reported in Figure 5.1 (left). The DE MNP samples could not be directly compared to the controls because the addition of NPs increased the turbidity of the solution which directly affects the OD_{600}, taken at 0 hr after DE MNP addition (as seen by the size discrepancy of the means between NPs and controls in Figure 5.1 (left)).

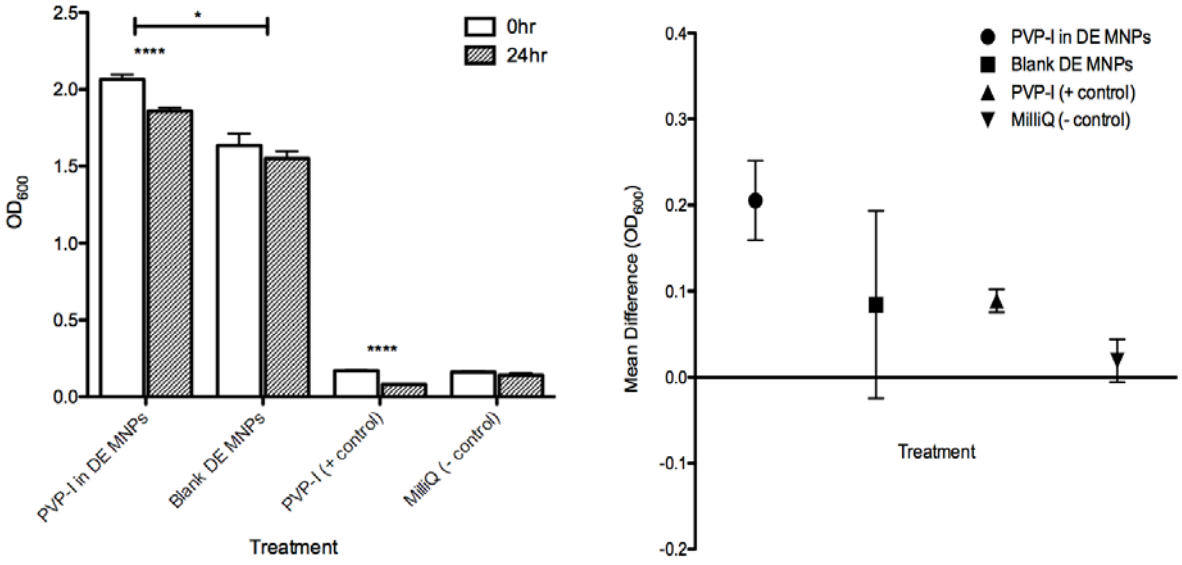

Figure 5.1 OD_{600} of Treatments at 0hr and 24hr (left) and 95% confidence interval (right) of bactericidal effects of PVP-I loaded DE MNPs on Escherichia coli; n = 7 ± s.e.

The confidence interval shown in Figure 5.1 (right) indicates the range of the true mean is within 95%. The standard error of the mean tells us how narrow/wide the variance is, with the lack of overlap to include zero indicating statistically different population medians at the 5% level of significance.

Bactericidal activity of PVP-I loaded DE MNPs suggests that 1% w/v of PVP-I is sufficient at eradicating a bacterial culture. Current formulations such as Betadine® use 5%w/v PVP-I for treatment of ocular infection due to rapid clearance [117]. Improving the mucoadhesion of DE MNPs *in vivo* insinuates that the amount of PVP-I currently used in ocular formulations can be reduced and just as effective in application.

Chapter 6
Conclusions & Future Work

6.1 Conclusions

Research conducted in the Frank Gu Research Group suggests that NP drug carriers are capable of circumventing corneal clearance mechanisms by manipulating the surface functionalization of polymeric nanoparticles (NPs) such that they can interact with the ocular mucosa. In view of this background, this thesis was aimed at exploring the potential of mucoadhesive NPs (MNPs) to encapsulate hydrophilic drugs in the core of the NP, while maintaining mucoadhesive functionality in the shell of the NP. We developed a novel approach to formulate a double emulsion mucoadhesive nanoparticle (DE MNP) system to deliver hydrophilic molecules.

Double emulsions allow us to generate a vesicle-like structure of hydrophilic interior and hydrophilic exterior and have been successful as nanoparticle drug carriers in the past. Most double emulsions utilize PLGA to make up the primary emulsion because it is a biodegradable and biocompatible polymer that has the ability to degrade into non-toxic by-products (lactic acid and glycolic acid) that are metabolized by the human body. The novelty in the DE MNP method involves using PLA-Dex-PBA in the outer emulsion, rather than common stabilizers such as PVA and Tween. The amphiphilic characteristics of PLA-Dex-PBA will arrange on the surface of PLGA emulsions with PLA facing the oil phase and Dex-PBA facing the exterior of the particle, making up the surface of DE MNPs. The PBA moieties on the surface of DE MNPs can covalently target the sialic acid moieties that are abundant on the ocular mucous membrane and avoid rapid clearance. DE MNPs form the foundation of the ocular drug delivery platform developed in this thesis, using fluorescein isothiocyanate dextran (FITC-Dex), a commercially used fluorescent dye, as the model drug to determine the capability of DE MNPs to encapsulate and release hydrophilic molecules. DE MNPs were first evaluated for size and morphology. They demonstrated sizes in the sub-200 nm range, nearly double the size of PLA-Dex-PBA MNP micelles. Their spherical shell/vesicle conformation was confirmed by static light scattering and TEM, and remained stable and unchanged with the addition of model FITC-Dex. DE MNPs demonstrated encapsulation of FITC-Dex up to 87 wt%, and sustained release for up to 7 days *in vitro*, showing their potential as a long-term eye drop delivery platform.

An *in vitro* mucoadhesion study as a proof of concept demonstration of PBA on DE MNPs' surfaces was demonstrated by studying the binding kinetics of PBA to sialic acid through the Stern-Volmer equation. The K_A value for DE MNPs with sialic acid was determined to be 107.83 M^{-1}, which was far higher than the literature values for PBA-SA. This gave confidence to the presence of PBA on the surface of DE MNPs. Next, we proceeded to attempt to demonstrate this mucoadhesion using *in vivo*

models. FITC-Dex was encapsulated in the NPs and administered to rabbit eyes to track its ocular retention. FITC-Dex delivered DE MNPs showed ocular retention for no longer than 3 hours on rabbit eyes; this trend was also seen for free FITC-Dex.

Povidone-Iodine (PVP-I), an inexpensive and commercially available drug commonly used to treat ocular bacterial infections, was encapsulated and evaluated for bactericidal activity upon release from DE MNPs. DE MNPs revealed that that encapsulation of the drug did not change the properties of the drug, and also confirmed that the amount of drug being encapsulated (1% w/v) in DE MNPs, is a sufficient concentration to elicit antimicrobial activity, and better than current formulations such as Betadine® which uses 5%w/v PVP-I for treatment of ocular infection.

This thesis demonstrated the development process of DE MNPs as topical ocular drug delivery systems for hydrophilic drugs. DE MNPs demonstrated delivery of a clinically relevant dosage of PVP-I, controlled release of therapeutics over prolonged period of time, and mucoadhesive properties *in vitro*. These DE mucoadhesive NPs show significant promise as a long-term topical ocular hydrophilic drug delivery system that significantly reduces the dose and the administration frequency of the eye drops while minimizing side effects.

6.2 Recommendation for Future Work

The research objectives outlined in section 1.2 were met through this body of work, and paved the way for future studies. The next step for assessing DE MNPs' viability as mucoadhesive ocular delivery agents will be to further characterize the surface of these particles. Studying the surface of DE MNPs is critical for their success as mucoadhesive drug delivery agents. It is clear that PBA is on the surface of DE MNPs because its fluorescence is quenched in the presence of SA, however, mucoadhesion was not seen *in vivo* and this may be because of the large size and strongly anionic surface of DE MNPs. We hypothesize that this is due to SPAN80 migrating to the surface, however this is merely speculation. This data should be furthered with more replicates of the binding study, first, to see if a more linear relationship can be achieved, then, optimization of DE MNP process parameters. This would help determine the contributing factors to the anionic surface charge observed. Furthermore, *in vivo* studies should be repeated after the former steps are taken, to determine DE MNPs' bioavailability on the ocular surface. Theoretically, DE MNPs should be able to avoid rapid clearance because of their mucoadhesive capabilities. Finally, in-depth analysis should be done on DE MNPs using a real drug rather than a model drug. Converting all the studies conducted using the model drug, using a hydrophilic antimicrobial agent that is easier to characterize than PVP-I, like ciprofloxacin, would conclusively reveal the potential of DE MNPs as hydrophilic ocular drug delivery systems.

References

[1] A. Mandal, D. Pal, V. Agrahari, H. M. Trinh, M. Joseph, and A. K. Mitra, "Ocular delivery of proteins and peptides: Challenges and novel formulation approaches," *Adv. Drug Deliv. Rev.*, 2018.

[2] S. Liu, L. Jones, and F. X. Gu, "Nanomaterials for Ocular Drug Delivery," *Macromol. Biosci.*, vol. 12, no. 5, pp. 608–620, 2012.

[3] J. Alvarez-trabado, Y. Diebold, and A. Sanchez, "Designing lipid nanoparticles for topical ocular drug delivery," *Int. J. Pharm.*, vol. 532, no. 1, pp. 204–217, 2017.

[4] B. Yavuz, S. B. Pehlivan, and N. Unlu, "Dendrimeric systems and their applications in ocular drug delivery.," *ScientificWorldJournal.*, vol. 2013, p. 732340, 2013.

[5] H. -U Schenck, P. Simak, and E. Haedicke, "Structure of polyvinylpyrrolidone-iodine (povidone-iodine)," *J. Pharm. Sci.*, vol. 68, no. 12, pp. 1505–1509, 1979.

[6] N. Kuno and S. Fujii, "Recent advances in ocular drug delivery systems," *Polymers (Basel).*, vol. 3, no. 1, pp. 193–221, 2011.

[7] R. Gaudana, H. K. Ananthula, A. Parenky, and A. K. Mitra, "Ocular Drug Delivery," *AAPS J.*, vol. 12, no. 3, pp. 348–360, 2010.

[8] S. Liu, L. Jones, and F. X. Gu, "Development of Mucoadhesive Drug Delivery System Using Phenylboronic Acid Functionalized Poly(D,L-lactide)-b-Dextran Nanoparticles," *Macromol. Biosci.*, vol. 12, no. 12, pp. 1622–1626, 2012.

[9] T. Peck, S. Hill, and M. Williams, "Drug passage across the cell membrane," *Pharmacol. Anaesth. Intensive Care, third Ed.*, pp. 1–10, 2008.

[10] S. Mitragotri, P. A. Burke, and R. Langer, "Overcoming the challenges in administering biopharmaceuticals: Formulation and delivery strategies," *Nat. Rev. Drug Discov.*, vol. 13, no. 9, pp. 655–672, 2014.

[11] H. Kimura and Y. Ogura, "Biodegradable polymers for ocular drug delivery.," *Ophthalmologica.*, vol. 215, no. 3, pp. 143–55, 2012.

[12] S. Cohen, T. Yoshioka, M. Lucarelli, L. H. Hwang, and R. Langer, "Controlled delivery systems for proteins based on poly(lactic/glycolic acid) microspheres.," *Pharmaceutical research*, vol. 8, no. 6. pp. 713–720, 1991.

[13] L. L. Mitic, C. M. Van Itallie, and J. M. Anderson, "Molecular physiology and pathophysiology of tight junctions I. Tight junction structure and function: lessons from mutant animals and proteins.," *Am. J. Physiol. Gastrointest. Liver Physiol.*, vol. 279, no. 2, pp. G250-4, 2000.

[14] Y. Tao, X. Li, Y. Jiang, X. Bai, B. Wu, and J. Dong, "Diffusion of macromolecule through retina

after experimental branch retinal vein occlusion and estimate of intraretinal barrier.," *Curr. Drug Metab.*, vol. 8, pp. 151–156, 2007.

[15] R. Agarwal *et al.*, "Liposomes in topical ophthalmic drug delivery: an update," *Drug Deliv.*, vol. 23, no. 4, pp. 1075–1091, 2016.

[16] A. Jensen, "Acta ophthalmologica vol. 4 3 1965," *Acta Ophthalmol.*, vol. 4, pp. 802–807, 1965.

[17] J. Barar, A. R. Javadzadeh, and Y. Omidi, "Ocular novel drug delivery: impacts of membranes and barriers," *Expert Opin. Drug Deliv.*, vol. 5, no. 5, pp. 567–581, 2008.

[18] P. Saha, K. J. Kim, and V. H. L. Lee, "A primary culture model of rabbit conjunctival epithelial cells exhibiting tight barrier properties," *Curr. Eye Res.*, vol. 15, no. 12, pp. 1163–1169, 1996.

[19] J. Ambati and A. P. Adamis, "Transscleral drug delivery to the retina and choroid," *Prog. Retin. Eye Res.*, vol. 21, no. 2, pp. 145–151, 2002.

[20] M. W. Mann and D. R. Berk, *Handbook of*. 2009.

[21] S. Raghava, M. Hammond, and U. B. Kompella, "Periocular routes for retinal drug delivery," *Expert Opin. Drug Deliv.*, vol. 1, no. 1, pp. 99–114, 2004.

[22] J. Cunha-Vaz, "The blood-ocular barriers," *Surv. Ophthalmol.*, vol. 23, no. 5, pp. 279–296, 1979.

[23] C. M. Kumar, H. Eid, and C. Dodds, "Sub-Tenon's anaesthesia: Complications and their prevention," *Eye*, vol. 25, no. 6, pp. 694–703, 2011.

[24] R. C. Nagarwal, S. Kant, P. N. Singh, P. Maiti, and J. K. Pandit, "Polymeric nanoparticulate system: A potential approach for ocular drug delivery," *J. Control. Release*, vol. 136, no. 1, pp. 2–13, 2009.

[25] M. Konishi, K. Kawamoto, M. Izumikawa, H. Kuriyama, and T. Yamashita, "Gene transfer into guinea pig cochlea using adeno-associated virus vectors.," *J. Gene Med.*, vol. 10, no. 6, pp. 610–618, 2008.

[26] E. Ron, T. Turek, E. Mathiowitz, M. Chasin, M. Hageman, and R. Langer, "Controlled release of polypeptides from polyanhydrides.," *Proc. Natl. Acad. Sci. U. S. A.*, vol. 90, no. 9, pp. 4176–4180, 1993.

[27] M. E. Davis and M. E. Brewster, "Cyclodextrin-based pharmaceutics: Past, present and future," *Nat. Rev. Drug Discov.*, vol. 3, no. 12, pp. 1023–1035, 2004.

[28] H. Kim, S. B. Robinson, and K. G. Csaky, "Investigating the movement of intravitreal human serum albumin nanoparticles in the vitreous and retina," *Pharm. Res.*, vol. 26, no. 2, pp. 329–337, 2009.

[29] A. Hayashi, A. Naseri, M. E. Pennesi, and E. De Juan, "Subretinal delivery of immunoglobulin G with gold nanoparticles in the rabbit eye," *Jpn. J. Ophthalmol.*, vol. 53, no. 3, pp. 249–256, 2009.

[30] B. Mahaling and D. S. Katti, "Physicochemical properties of core-shell type nanoparticles govern

their spatiotemporal biodistribution in the eye," *Nanomedicine Nanotechnology, Biol. Med.*, vol. 12, no. 7, pp. 2149–2160, 2016.

[31] B. Senturk, M. O. Cubuk, M. C. Ozmen, B. Aydin, M. O. Guler, and A. B. Tekinay, "Inhibition of VEGF mediated corneal neovascularization by anti-angiogenic peptide nanofibers," *Biomaterials*, vol. 107, pp. 124–132, 2016.

[32] R. Bodmeier and J. W. McGinity, "The Preparation and Evaluation of Drug-Containing Poly(dl-lactide) Microspheres Formed by the Solvent Evaporation Method," *Pharmaceutical Research: An Official Journal of the American Association of Pharmaceutical Scientists*, vol. 4, no. 6. pp. 465–471, 1987.

[33] W. Hachicha, L. Kodjikian, and H. Fessi, "Preparation of vancomycin microparticles: Importance of preparation parameters," *Int. J. Pharm.*, vol. 324, no. 2, pp. 176–184, 2006.

[34] O. Karal-Yilmaz, M. Serhatli, K. Baysal, and B. M. Baysal, "Preparation and in vitro characterization of vascular endothelial growth factor (VEGF)-loaded poly(D,L-lactic-co-glycolic acid) microspheres using a double emulsion/solvent evaporation technique," *J. Microencapsul.*, vol. 28, no. 1, pp. 46–54, 2011.

[35] H. Wang *et al.*, "Hyaluronic acid-decorated dual responsive nanoparticles of Pluronic F127, PLGA, and chitosan for targeted co-delivery of doxorubicin and irinotecan to eliminate cancer stem-like cells," *Biomaterials*, vol. 72, pp. 74–89, 2015.

[36] S. S. Feng *et al.*, "Vitamin E TPGS-emulsified poly(lactic-co-glycolic acid) nanoparticles for cardiovascular restenosis treatment," *Nanomedicine*, vol. 2, no. 3, pp. 333–344, 2007.

[37] K. Yoncheva, J. Vandervoort, and A. Ludwig, "Development of mucoadhesive poly(lactide-co-glycolide) nanoparticles for ocular application," *Pharm. Dev. Technol.*, vol. 16, no. 1, pp. 29–35, 2011.

[38] E. Chang, A. J. Mcclellan, W. J. Farley, D. Li, and C. Stephen, "Biodegradable PLGA-Based Drug Delivery Systems For Modulating Ocular Surface Disease under Experimental Murine Dry Eye," *J. Clin. Exp. Ophthamology*, vol. 2, no. 11, pp. 1–13, 2013.

[39] Y. Wang, A. Rajala, and R. V. S. Rajala, "Lipid nanoparticles for ocular gene delivery," *J. Funct. Biomater.*, vol. 6, no. 2, pp. 379–394, 2015.

[40] I. Journal, "Liposomes and nanotechnology in drug development : Focus on ocular targets Liposomes and nanotechnology in drug development : focus on ocular targets," no. February, pp. 495–504, 2013.

[41] S. Mashaghi, T. Jadidi, G. Koenderink, and A. Mashaghi, *Lipid nanotechnology*, vol. 14, no. 2. 2013.

[42] D. Lombardo, P. Calandra, D. Barreca, S. Magazù, and M. Kiselev, "Soft Interaction in Liposome

Nanocarriers for Therapeutic Drug Delivery," *Nanomaterials*, vol. 6, no. 7, p. 125, 2016.

[43] M. S. Nagarsenker, V. Y. Londhe, and G. D. Nadkarni, "Preparation and evaluation of liposomal formulations of tropicamide for ocular delivery," *Int. J. Pharm.*, vol. 190, no. 1, pp. 63–71, 1999.

[44] R. M. Hathout, S. Mansour, N. D. Mortada, and A. S. Guinedi, "Liposomes as an ocular delivery system for acetazolamide: In vitro and in vivo studies," *AAPS PharmSciTech*, vol. 8, no. 1, pp. E1–E12, 2007.

[45] T. Lian and R. J. Ho, "Trends and developments in liposome drug delivery systems.," *J. Pharm. Sci.*, vol. 90, no. 6, pp. 667–680, 2001.

[46] N. Ferrara, L. Damico, H. Lowman, and R. Kim, "Development of Ranibizumab, an Anti–Vascular Endothelial Growth Factor Antigen Binding Fragment, As Therapy for Neovascular Age-Related Macular Degeneration," *J. Retin. Vitr. Dis.*, vol. 26, no. 8, pp. 859–870, 2006.

[47] R. M. Rich *et al.*, "Short-term safety and efficacy of intravitreal bevacizumab (Avastin) for neovascular age-related macular degeneration," *Retina*, vol. 26, no. 5, pp. 495–511, 2006.

[48] M. E. Iliev, D. Domig, U. Wolf-Schnurrbursch, S. Wolf, and G. M. Sarra, "Intravitreal Bevacizumab (Avastin®) in the Treatment of Neovascular Glaucoma," *Am. J. Ophthalmol.*, vol. 142, no. 6, pp. 1054–1056, 2006.

[49] R. L. Avery *et al.*, "Intravitreal Bevacizumab (Avastin) in the Treatment of Proliferative Diabetic Retinopathy," *Ophthalmology*, vol. 113, no. 10, 2006.

[50] M. Abrishami, S. Zarei-Ghanavati, D. Soroush, M. Rouhbakhsh, M. R. Jaafari, and B. Malaekeh-Nikouei, "Preparation, characterization, and in vivo evaluation of nanoliposomes-encapsulated bevacizumab (avastin) for intravitreal administration," *Retina*, vol. 29, no. 5, pp. 699–703, 2009.

[51] G. Swathi, N. L. Prasanthi, S. S. Manikiran, and N. Ramarao, "ChemInform Abstract: Solid Lipid Nanoparticles: Colloidal Carrier Systems for Drug Delivery," *ChemInform*, vol. 43, no. 2, p. no-no, 2012.

[52] R. Cavalli, M. R. Gasco, P. Chetoni, S. Burgalassi, and M. F. Saettone, "Solid lipid nanoparticles (SLN) as ocular delivery system for tobramycin," *Int. J. Pharm.*, vol. 238, no. 1–2, pp. 241–245, 2002.

[53] A. J. Almeida and E. Souto, "Solid lipid nanoparticles as a drug delivery system for peptides and proteins," *Adv. Drug Deliv. Rev.*, vol. 59, no. 6, pp. 478–490, 2007.

[54] A. Edwards and M. R. Prausnitz, "Predicted permeability of the cornea to topical drugs," *Pharm. Res.*, vol. 18, no. 11, pp. 1497–1508, 2001.

[55] S. H. Kim *et al.*, "Assessment of subconjunctival and intrascleral drug delivery to the posterior segment using dynamic contrast-enhanced magnetic resonance imaging," *Investig. Ophthalmol. Vis. Sci.*, vol. 48, no. 2, pp. 808–814, 2007.

[56] S. Nakao, A. Hafezi-Moghadam, and T. Ishibashi, “Lymphatics and lymphangiogenesis in the eye,” *J. Ophthalmol.*, vol. 2012, 2012.

[57] M. R. Prausnitz and J. S. Noonan, “Permeability of cornea, sclera, and conjunctiva: A literature analysis for drug delivery to the eye,” *J. Pharm. Sci.*, vol. 87, no. 12, pp. 1479–1488, 1998.

[58] A. W. Du and M. H. Stenzel, “Drug carriers for the delivery of therapeutic peptides,” *Biomacromolecules*, vol. 15, no. 4, pp. 1097–1114, 2014.

[59] C. Peetla and V. Labhasetwar, “Effect of molecular structure of cationic surfactants on biophysical interactions of surfactant-modified nanoparticles with a model membrane and cellular uptake,” *Langmuir*, vol. 25, no. 4, pp. 2369–2377, 2009.

[60] A. M. De Campos, A. Sánchez, R. Gref, P. Calvo, and M. J. Alonso, “The effect of a PEG versus a chitosan coating on the interaction of drug colloidal carriers with the ocular mucosa,” *Eur. J. Pharm. Sci.*, vol. 20, no. 1, pp. 73–81, 2003.

[61] E. Başaran, M. Demirel, B. Sirmagül, and Y. Yazan, “Cyclosporine-A incorporated cationic solid lipid nanoparticles for ocular delivery,” *J. Microencapsul.*, vol. 27, no. 1, pp. 37–47, 2010.

[62] A. Seyfoddin, J. Shaw, and R. Al-Kassas, “Solid lipid nanoparticles for ocular drug delivery,” *Drug Deliv.*, vol. 17, no. 7, pp. 467–489, 2010.

[63] F. Sousa, P. Castro, P. Fonte, P. J. Kennedy, M. T. Neves-Petersen, and B. Sarmento, “Nanoparticles for the delivery of therapeutic antibodies: Dogma or promising strategy?,” *Expert Opin. Drug Deliv.*, vol. 14, no. 10, pp. 1163–1176, 2017.

[64] J. Shen, Y. Deng, X. Jin, Q. Ping, Z. Su, and L. Li, “Thiolated nanostructured lipid carriers as a potential ocular drug delivery system for cyclosporine A: Improving in vivo ocular distribution,” *Int. J. Pharm.*, vol. 402, no. 1–2, pp. 248–253, 2010.

[65] C. C. Lee, J. A. MacKay, J. M. J. Fréchet, and F. C. Szoka, “Designing dendrimers for biological applications,” *Nat. Biotechnol.*, vol. 23, no. 12, pp. 1517–1526, 2005.

[66] A. Guzman-Aranguez and P. Argüeso, “Structure and biological roles of mucin-type O-glycans at the ocular surface,” *Ocul. Surf.*, vol. 8, no. 1, pp. 8–17, 2010.

[67] S. P. Kambhampati and R. M. Kannan, “Dendrimer Nanoparticles for Ocular Drug Delivery,” *J. Ocul. Pharmacol. Ther.*, vol. 29, no. 2, pp. 151–165, 2013.

[68] W. Yao *et al.*, “Preparation and characterization of puerarindendrimer complexes as an ocular drug delivery system,” *Drug Dev. Ind. Pharm.*, vol. 36, no. 9, pp. 1027–1035, 2010.

[69] R. Tarallo *et al.*, “Dendrimers functionalized with membrane-interacting peptides for viral inhibition,” *Int. J. Nanomedicine*, vol. 8, pp. 521–534, 2013.

[70] A. Gothwal, I. Khan, and U. Gupta, “Polymeric Micelles: Recent Advancements in the Delivery of Anticancer Drugs,” *Pharm. Res.*, vol. 33, no. 1, pp. 18–39, 2016.

[71] A. Mandal, R. Bisht, I. D. Rupenthal, and A. K. Mitra, “Polymeric micelles for ocular drug delivery: From structural frameworks to recent preclinical studies,” *J. Control. Release*, vol. 248, pp. 96–116, 2017.

[72] S. C. Owen, D. P. Y. Chan, and M. S. Shoichet, “Polymeric micelle stability,” *Nano Today*, vol. 7, no. 1, pp. 53–65, 2012.

[73] C. Deng, Y. Jiang, R. Cheng, F. Meng, and Z. Zhong, “Biodegradable polymeric micelles for targeted and controlled anticancer drug delivery: Promises, progress and prospects,” *Nano Today*, vol. 7, no. 5, pp. 467–480, 2012.

[74] Y. Ali and K. Lehmussaari, “Industrial perspective in ocular drug delivery,” *Adv. Drug Deliv. Rev.*, vol. 58, no. 11, pp. 1258–1268, 2006.

[75] a P. Gadad, P. S. Chandra, P. M. Dandagi, and V. S. Mastiholimath, “Moxifloxacin Loaded Polymeric Nanoparticles for Sustained Ocular Drug Delivery,” *J. Pharm. Sci.*, pp. 1727–1734, 2012.

[76] X. Yuan *et al.*, “Ocular drug delivery nanowafer with enhanced therapeutic efficacy,” *ACS Nano*, vol. 9, no. 2, pp. 1749–1758, 2015.

[77] Y. Wang, P. Li, and L. Kong, “Chitosan-Modified PLGA Nanoparticles with Versatile Surface for Improved Drug Delivery,” *AAPS PharmSciTech*, vol. 14, no. 2, pp. 585–592, 2013.

[78] S. Mao, Y. Shi, L. Li, J. Xu, A. Schaper, and T. Kissel, “Effects of process and formulation parameters on characteristics and internal morphology of poly(d,l-lactide-co-glycolide) microspheres formed by the solvent evaporation method,” *Eur. J. Pharm. Biopharm.*, vol. 68, no. 2, pp. 214–223, 2008.

[79] P. Li, Y. Wang, F. Zeng, L. Chen, Z. Peng, and L. X. Kong, “Synthesis and characterization of folate conjugated chitosan and cellular uptake of its nanoparticles in HT-29 cells,” *Carbohydr. Res.*, vol. 346, no. 6, pp. 801–806, 2011.

[80] L. V. I. A. Folate-peg-chol, W. Guo, T. Lee, J. Sudimack, and R. J. Lee, “RECEPTOR-SPECIFIC DELIVERY OF,” vol. 10, pp. 179–195, 2000.

[81] Croda Europe Ltd, “Span and Tween,” *Www.Croda.Com/Europe*, vol. 44, no. 0, pp. 6–11, 2009.

[82] L. Duxfield *et al.*, “Ocular delivery systems for topical application of anti-infective agents,” *Drug Dev. Ind. Pharm.*, vol. 42, no. 1, pp. 1–11, 2016.

[83] H. Search, C. Journals, A. Contact, M. Iopscience, and I. P. Address, “Emulsions : basic principles Emulsions : basic principles,” *Reports Prog. Phys.*, vol. 969, no. 62, p. 969, 1999.

[84] N. Sharma, P. Madan, and S. Lin, “Effect of process and formulation variables on the preparation of parenteral paclitaxel-loaded biodegradable polymeric nanoparticles: A co-surfactant study,” *Asian J. Pharm. Sci.*, vol. 11, no. 3, pp. 404–416, 2016.

[85] S. Mao, J. Xu, C. Cai, O. Germershaus, A. Schaper, and T. Kissel, “Effect of WOW process parameters on morphology and burst release of FITC-dextran loaded PLGA microspheres,” *Int. J. Pharm.*, vol. 334, no. 1–2, pp. 137–148, 2007.

[86] K. F. Pistel, T. Kissel, “Effects of salt addition on the microencapsulation of proteins using W/O/W double emulsion technique,” *J. Microencapsul.*, vol. 17, no. 4, pp. 467–483, 2000.

[87] J. Santos, N. Calero, L. A. Trujillo-Cayado, M. C. Garcia, and J. Muñoz, “Assessing differences between Ostwald ripening and coalescence by rheology, laser diffraction and multiple light scattering,” *Colloids Surfaces B Biointerfaces*, vol. 159, pp. 405–411, 2017.

[88] R. R. Hegde, A. Verma, and A. Ghosh, “Microemulsion: New Insights into the Ocular Drug Delivery,” *ISRN Pharm.*, vol. 2013, pp. 1–11, 2013.

[89] P. a Hassan, S. Rana, and G. Verma, “Making sense of brownian motion: colloid characterization by dynamic light scattering.,” *Langmuir*, vol. 31, no. 1, pp. 3–12, 2015.

[90] M. Sandor, D. Enscore, P. Weston, and E. Mathiowitz, “Effect of protein molecular weight on release from micron-sized PLGA microspheres,” *J. Control. Release*, vol. 76, no. 3, pp. 297–311, 2001.

[91] A. D. Switzer, *Measuring and Analyzing Particle Size in a Geomorphic Context*, vol. 14, no. March 2013. 2013.

[92] J. Hotz and W. Meier, “Vesicle-Templated Polymer Hollow Spheres,” *Langmuir*, vol. 14, no. 5, pp. 1031–1036, 1998.

[93] J. Vandervoort and A. Ludwig, “Biocompatible stabilizers in the preparation of PLGA nanoparticles: A factorial design study,” *Int. J. Pharm.*, vol. 238, no. 1–2, pp. 77–92, 2002.

[94] Y. Wang, X. Zhang, Y. Han, C. Cheng, and C. Li, “PH- and glucose-sensitive glycopolymer nanoparticles based on phenylboronic acid for triggered release of insulin,” *Carbohydr. Polym.*, vol. 89, no. 1, pp. 124–131, 2012.

[95] S. Honary and F. Zahir, “Effect of Zeta Potential on the Properties of Nano - Drug Delivery Systems - A Review (Part 2),” *Trop. J. Pharm. al Res.*, vol. 12, no. 2, pp. 265–273, 2013.

[96] S. Darwich, K. Mougin, and H. Haidara, “From highly ramified, large scale dendrite patterns of drying ‘alginate/Au NPs’ solutions to capillary fabrication of lab-scale composite hydrogel microfibers,” *Soft Matter*, vol. 8, no. 4, pp. 1155–1162, 2012.

[97] U. E. M. Stain, “A Substitute for Uranyl Acetate.”

[98] N. F. Cheville and J. Stasko, “Techniques in Electron Microscopy of Animal Tissue,” *Vet. Pathol.*, vol. 51, no. 1, pp. 28–41, 2014.

[99] Y. Y. Yang, T. S. Chung, and N. Ping Ng, “Morphology, drug distribution, and in vitro release profiles of biodegradable polymeric microspheres containing protein fabricated by double-

emulsion solvent extraction/evaporation method," *Biomaterials*, vol. 22, no. 3, pp. 231–241, 2001.

[100] T. Painbeni, M. C. Venier-Julienne, and J. P. Benoit, "Internal morphology of poly(D,L-lactide-co-glycolide) BCNU-loaded microspheres. Influence on drug stability," *Eur. J. Pharm. Biopharm.*, vol. 45, no. 1, pp. 31–39, 1998.

[101] D. R. Brackenridge, "United States Patent," vol. 2, no. 12, 1992.

[102] S. Honary, M. Jahanshahi, P. Golbayani, P. Ebrahimi, and K. Ghajar, "Doxorubicin-Loaded Albumin Nanoparticles: Formulation and Characterization," *J. Nanosci. Nanotechnol.*, vol. 10, no. 11, pp. 7752–7757, 2010.

[103] N. Csaba, M. Garcia-Fuentes, and M. J. Alonso, "The performance of nanocarriers for transmucosal drug delivery.," *Expert Opin. Drug Deliv.*, vol. 3, no. 4, pp. 463–478, 2006.

[104] Y. Suzuki *et al.*, "Sialic Acid Species as a Determinant of the Host Range of Influenza A Viruses," *J. Virol.*, vol. 74, no. 24, pp. 11825–11831, 2000.

[105] S. Liu *et al.*, "Prolonged ocular retention of mucoadhesive nanoparticle eye drop formulation enables treatment of eye diseases using significantly reduced dosage," *Mol. Pharm.*, vol. 13, no. 9, pp. 2897–2905, 2016.

[106] R. Dinarvand, N. Sepehri, S. Manoochehri, H. Rouhani, and F. Atyabi, "Polylactide-co-glycolide nanoparticles for controlled delivery of anticancer agents.," *Int. J. Nanomedicine*, vol. 6, pp. 877–895, 2011.

[107] B. Pappin, M. J., and T. A., "Boron-Carbohydrate Interactions," *Carbohydrates - Compr. Stud. Glycobiol. Glycotechnol.*, 2012.

[108] H. Otsuka, E. Uchimura, H. Koshino, T. Okano, and K. Kataoka, "Anomalous binding profile of phenylboronic acid with N-acetylneuraminic acid (Neu5Ac) in aqueous solution with varying pH," *J. Am. Chem. Soc.*, vol. 125, no. 12, pp. 3493–3502, 2003.

[109] C. Cheng, X. Zhang, Y. Wang, L. Sun, and C. Li, "Phenylboronic acid-containing block copolymers: Synthesis, self-assembly, and application for intracellular delivery of proteins," *New J. Chem.*, vol. 36, no. 6, pp. 1413–1421, 2012.

[110] S. Deshayes *et al.*, "Phenylboronic acid-installed polymeric micelles for targeting sialylated epitopes in solid tumors," *J. Am. Chem. Soc.*, vol. 135, no. 41, pp. 15501–15507, 2013.

[111] K. Kur-Kowalska, M. Przybyt, P. Ziółczyk, P. Sowiński, and E. Miller, "Fluorescence properties of 3-amino phenylboronic acid and its interaction with glucose and ZnS:Cu quantum dots," *Spectrochim. Acta - Part A Mol. Biomol. Spectrosc.*, vol. 129, pp. 320–325, 2014.

[112] W. L. A. Brooks and B. S. Sumerlin, "Synthesis and Applications of Boronic Acid-Containing Polymers: From Materials to Medicine," *Chem. Rev.*, vol. 116, no. 3, pp. 1375–1397, 2016.

[113] K. Djanashvili, L. Frullano, and J. A. Peters, "Molecular recognition of sialic acid end groups by

phenylboronates," *Chem. - A Eur. J.*, vol. 11, no. 13, pp. 4010–4018, 2005.

[114] G. Springsteen and B. Wang, "A detailed examination of boronic acid-diol complexation," *Tetrahedron*, vol. 58, no. 26, pp. 5291–5300, 2002.

[115] V. V. Khutoryanskiy, "Advances in Mucoadhesion and Mucoadhesive Polymers," *Macromol. Biosci.*, vol. 11, no. 6, pp. 748–764, 2011.

[116] S. Nishitani, Y. Maekawa, and T. Sakata, "Understanding the Molecular Structure of the Sialic Acid-Phenylboronic Acid Complex by using a Combined NMR Spectroscopy and DFT Study: Toward Sialic Acid Detection at Cell Membranes," *ChemistryOpen*, vol. 7, no. 7, pp. 513–519, 2018.

[117] S. J. Isenberg and L. Apt, "The Ocular Application of Povidone-Iodine," *Community Eye Heal.*, vol. 16, no. 46, pp. 30–31, 2003.

[118] A. C. Ms, S. Rani, J. Dnb, V. Stephen, M. S. Dnb, and M. Chakrabarti, "Povidone – Iodine in O phthalmology," vol. XIX, no. 3, pp. 282–286.

[119] H. Schreier, G. Erdos, K. Reimer, B. König, W. König, and W. Fleischer, "Molecular effects of povidone-iodine on relevant microorganisms: An electron-microscopic and biochemical study," *Dermatology*, vol. 195, no. 2, pp. 111–116, 1997.

[120] A. Bolt, "Povidone-iodine," *Community Eye Heal.*, vol. 16, no. 48, p. 63, 2003.

[121] J. L. Zamora, "Chemical and microbiologic characteristics and toxicity of povidone-iodine solutions," *Am. J. Surg.*, vol. 151, no. 3, pp. 400–406, 1986.

[122] R. W. LACEY, "Antibacterial Activity of Povidone Iodine towards Non-sporing Bacteria," *J. Appl. Bacteriol.*, vol. 46, no. 3, pp. 443–449, 1979.

[123] H. Pan, Y. Zhang, G.-X. He, N. Katagori, and H. Chen, "A comparison of conventional methods for the quantification of bacterial cells after exposure to metal oxide nanoparticles," *BMC Microbiol.*, vol. 14, no. 1, p. 222, 2014.

Appendix A

Formulation	Diameter[a)] (nm)	PDI[b)]	R_g/R_h[c)]
Blank DE MNPs (immediate addition)	151	0.0480	0.916
Blank DE MNPs (retarded addition)	201	0.1270	1.73

Table 7.1 Characterization of blank DE MNPs after immediate addition and retarded addition and sonication of primary emulsion to 0.1% w/v PLA-Dex-PBA by (a) size, (b) polydispersity index, and (c) conformation; n = 1

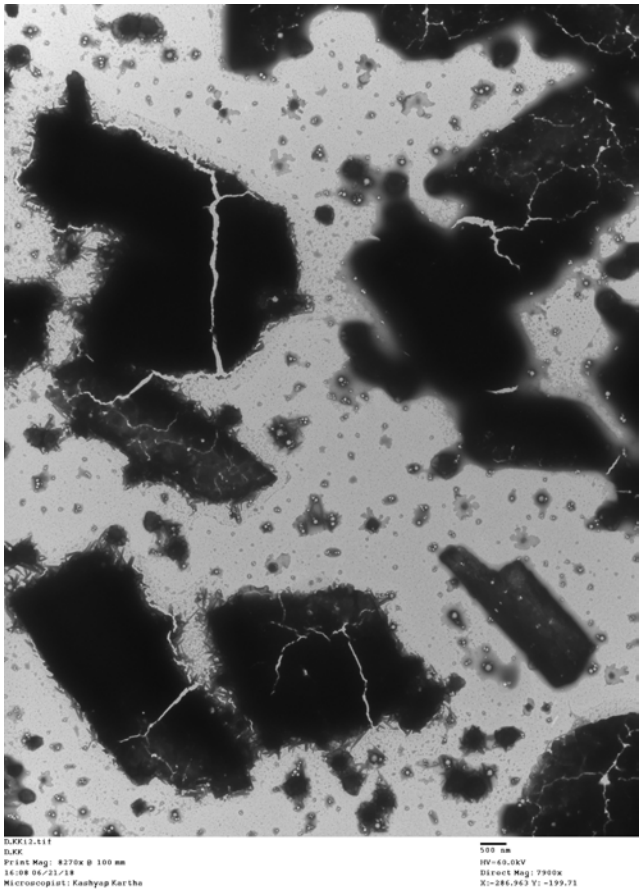

Figure 7.1 TEM of blank DE MNPs after retarded addition and sonication of primary emulsion to 0.1% w/v PLA-Dex-PBA

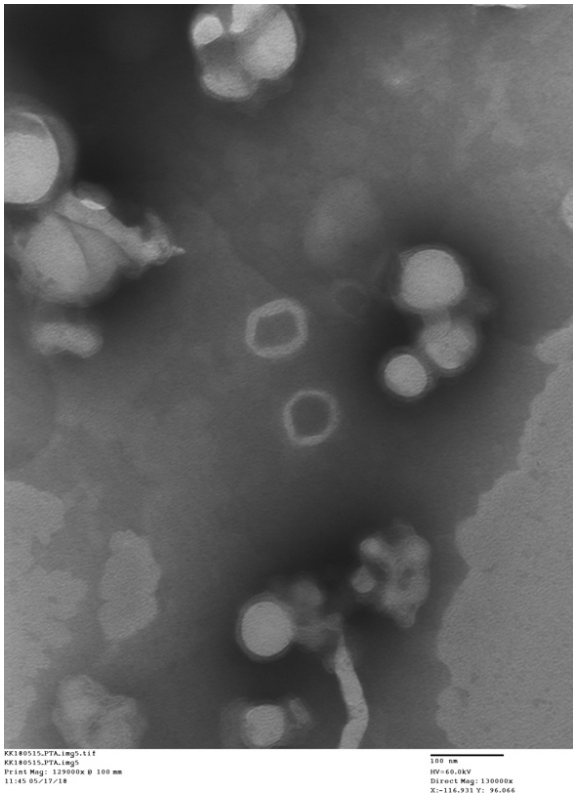

-

Figure 7.2 PTA loaded and stained DE MNPs

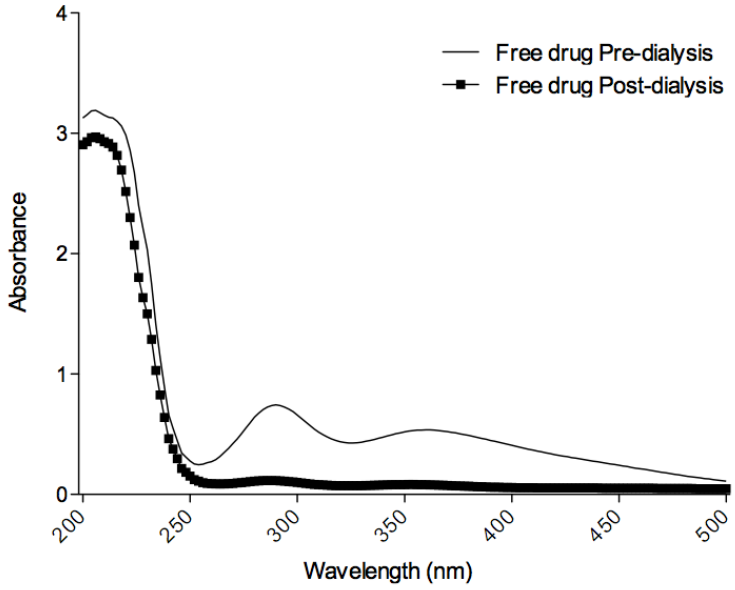

Figure 7.3 Free-Drug Dialysis Test for PVP-I to test how much Iodine is lost when PVP-I is in solution.